UNIVERSITÀ DEGLI STUDI
DI MODENA E REGGIO EMILIA

Ph.D. in "Molecular and Regenerative Medicine"

XXXIV Cycle

"Development of a tissue engineered 3D human hemi-cornea growing primary human keratinocytes on a biocompatible scaffold"

Candidate: Federica Maria Magrelli

Supervisor (Tutor): Professor Graziella Pellegrini

Coordinator of the PhD Course: Professor Michele De Luca

Index

Abstract

Corneal diseases are the most frequent causes of vision loss, second only to cataracts. According to the World Health Organization, more than 45 million people worldwide are bilaterally blind, and other 135 million individuals have severely impaired vision in both eyes [1].

In this perspective, tissue engineering (TE) for corneal replacement represents the new challenge, involving using natural substrates for TE corneal reconstruction. This leads to medical improvements and progress of the society, solving donor cornea problems and implementing social and economic values [2].

The cornea is the transparent interface between the eye and the external environment. It comprises three main cellular layers: the outermost stratified epithelium, a middle stroma, and the innermost endothelial layer. Two acellular collagenous interfaces are interposed between those cellular layers referred to as the Bowman's layer and the Descemet's membrane.

In case of widespread chemical burns or physical damages affecting the corneal epithelium, a partial or complete loss of stem cells (resident in the limbus zone) occurs, and bulbar conjunctival cells immediately spread towards the center of the eye to cover the wound (conjunctivalization process). A failure of the limbal function can result in the painful and blinding disease of Limbal Stem Cell Deficiency (LSCD). Studies on autologous cultures of limbal epithelial stem cells have been proven to permanently restore the corneal epithelium in patients characterized by LSCD and not treatable with standard surgical procedures [3]. However, if the damage is deeper and involves the stroma, the autologous cultured graft is insufficient. Thus, the most used options to restore visual acuity in stromal damage are the penetrating keratoplasty (PK) procedure and the lamellar keratoplasty. These procedures involve corneal transplantation with a full-thickness human donor cornea graft or part of it. However, these procedures should be overcome due to donor corneas shortage and significant complications of immunological rejection, glaucoma, and microbial keratitis, limiting success.

Thus, in an era of proposing new technologies and discovering new biomaterials, progresses in corneal cell culture and corneal TE can be performed both for basic scientific research and clinical application. The need for replacing the severe corneal stromal damage still needs to be addressed safely and innovatively and substituting a damaged cornea with clear biomaterials still represents an open challenge to give a safe, clear sight back to those who have not seen for a long time.

This project aims to test different innovative bio-engineered transparent materials and analyze the biocompatibility and growth of limbal stem cells onto their surface for scientific and clinical purposes. Thus, biocompatible materials resembling the natural cornea for transparency, architecture, stiffness, mechanical strength, and surface patterning will be considered stromal substitutes.

Previous research has identified a new, highly transparent scaffold with biomechanical properties resembling the human cornea, the crustaceous chitin [4]. This material revealed a stiffness mimicking the human cornea, as measured by atomic force microscopy (AFM). The β-chitin, in results, is made

up of different layers and, after treatments, it resembles the corneal stroma. Other great options evaluated include innovative collagen-like hydrogels [5]. These materials successfully mimic the function of full-length recombinant human collagen stroma useful for corneal implants.

Thus, this project merges the extensive knowledge on epithelial stem cells combined with new brilliant substrates alternatives to reconstruct a Hemi-cornea (i.e., epithelialized stroma), seeding primary human keratinocytes on biocompatible scaffolds. Then, the proposed tissue-engineered constructs are evaluated for their capability to maintain the differentiation program and the stem cell content. In conclusion, we aim to deliver this *in vitro* 3D corneal model for future investigation on common drugs, and in the future, as a clinical-grade cornea for autologous regeneration as a substitute for standard invasive procedures.

Sintesi

Secondo l'Organizzazione Mondiale della Sanità (OMS), le malattie della cornea sono la quarta causa di perdita della vista a livello globale. C'è una necessità universale sia per la cura oculare che per il ripristino dell'acuità oculare e nei decenni futuri la previsione rimane ancora critica. Le malattie degli occhi colpiscono almeno 2,2 miliardi di persone in tutto il mondo, sia per problemi visivi che per cecità totale. Tra questi, più di 1 miliardo rappresenta una disabilità visiva che deve ancora essere affrontata o che si sarebbe potuta evitare.

La cornea è l'interfaccia trasparente tra l'occhio e l'ambiente esterno e, a causa della sua posizione esterna, potrebbe essere danneggiata da lesioni e infezioni. In presenza di un danno stromale significativo, una delle tecniche più utilizzate per ripristinare l'acuità visiva è il trapianto di cornea allogenico (la procedura di cheratoplastica); in cui per il trapianto viene utilizzata una cornea di donatore umano come innesto. La cornea può essere sostituita nella sua totalità (cheratoplastica perforante) o in parte (cheratoplastica lamellare).

Questa procedura dovrebbe essere superata a causa della carenza di donatori e delle complicazioni legate al rigetto immunologico, al glaucoma e alla cheratite microbica, che ancora limitano il successo. Pertanto, una vasta gamma di biomateriali viene sempre più presa in considerazione come sostituto della procedura di cheratoplastica. L'intento è quello di trovare substrati naturali e biocompatibili per la ricostruzione corneale. Pertanto, è importante considerare la funzione e l'anatomia della cornea umana come precursori per la valutazione di una varietà di diversi biomateriali per la rigenerazione corneale.

Dunque, lo scopo di questo progetto è quello di ricostruire una cornea completamente autologa, coltivando cellule corneali umane primarie su scaffold biocompatibili. Grazie alla nostra precedente conoscenza ed esperienza sulla coltivazione e caratterizzazione di cellule staminali limbari, abbiamo innanzitutto analizzato la corretta adesione, colonizzazione e crescita dei cheratinociti limbari umani su diversi scaffold biocompatibili e trasparenti. Inoltre, poiché è importante che i nostri biomateriali abbiano proprietà specifiche utili per il trapianto clinico, abbiamo analizzato: l'origine naturale, la biocompatibilità e la biodegradabilità, in aggiunta a caratteristiche come la forza biomeccanica significativa e una trasparenza molto elevata. Pertanto, abbiamo esplorato queste caratteristiche per selezionare il miglior candidato per la ricostruzione corneale.

Infine, abbiamo ottimizzato anche le procedure per la standardizzazione. Infatti, abbiamo migliorato la realizzazione del nostro modello, controllando la semina cellulare e selezionando le caratteristiche appropriate degli scaffold naturali analizzati al fine di utilizzare, in futuro, questi biomateriali per test farmacologici *in vitro* o per scopi clinici.

Introduction

Corneal anatomy and physiology

The principle of ocular surface presented by Thoft and Friend in 1979 [6, 7] has been extensively recognized among the scientific community investigating the biology of the anterior part of the eye and the pathogenesis of the ocular surface disease [7]. This view, led to multiple developments and discoveries over the past 40 years. Based on numerous scientific progress, where animal testing was a crucial part of every study, a new line of research has developed and new technologies and discoveries are crucial to deeply examine the nature of the human corneal surface.

The function of the ocular surface system is to maintain and protect the smooth refractive surface of the cornea. This includes the surface and glandular epithelia of the cornea, conjunctiva, lacrimal gland, accessory lacrimal glands, and Meibomian gland, and their apical (tears) and basal (connective tissue) matrices, the eyelashes and the nasolacrimal duct. All those parts, are functionally linked by continuity of the epithelia, by innervation, and by the endocrine, vascular and immune systems [8].

The cornea is a transparent avascular tissue that acts as a structural barrier and protects the eye. Along with the tear film, it provides appropriate anterior refractive surface for the eye. Cornea contributes to two-third of the refractive power of the eye [9]. It is transparent and avascular, and it measures about 12 to 13mm in the vertical and horizontal diameters; the thickness is approximately 0.5mm at the center, increasing progressively toward the sclera [10, 11].

The cornea consists of five different layers. Three cellular layers are the epithelium, the stroma, and the endothelium, and two acellular collagenous interfaces are the Bowman's layer and the Descemet's membrane (Fig.1). The cornea's primary function is to focus most of the light entering the eye and to refract it. Together with the sclera, it acts as a barrier against damages (e.g., germs, dirt, chemicals). Each single layer has a function and all together they allow the refraction of light beams along with the lens to provide eyesight focusing on the retina. Eyes hydration comes anteriorly from the tears and posteriorly from the aqueous humor [12].

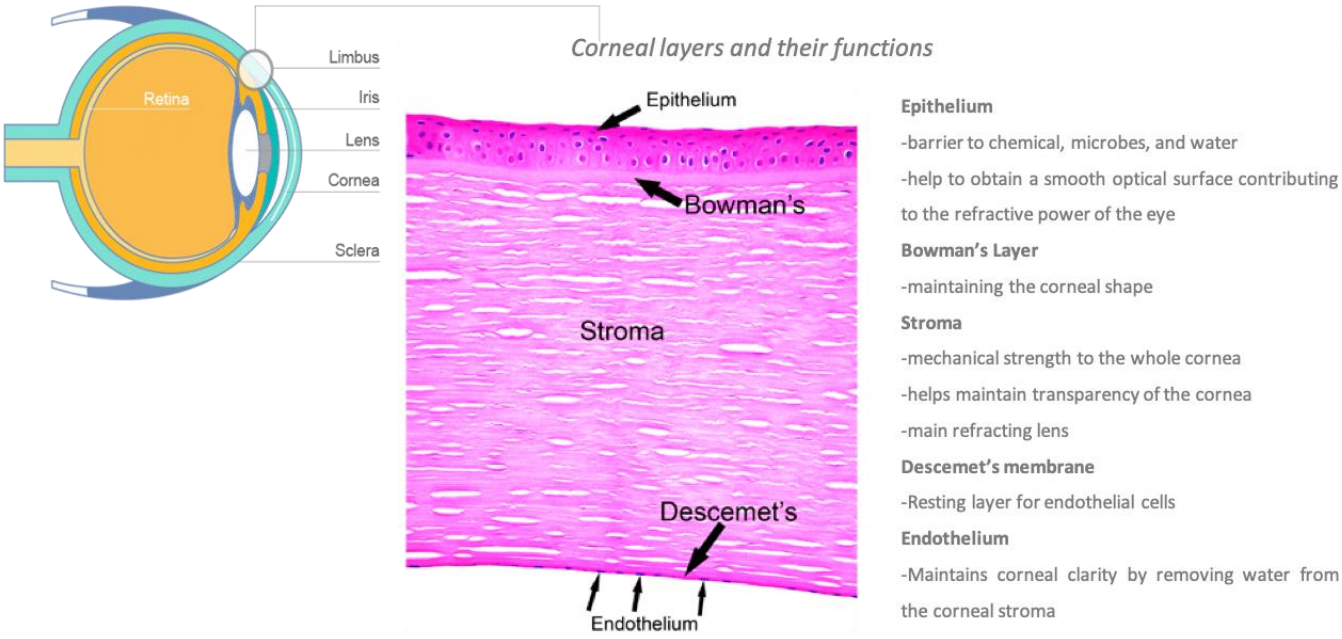

Fig.1 Overall structure of the eye, corneal layers, and their function

The epithelium

The corneal epithelium is the outer layer, essential for corneal transparency and that mainly contributes to create a biological barrier function for the eye. It is a stratified squamous tissue of 40-50um, representing the 10% of the final corneal thickness. Also, in association with the tear film, represents a smooth interface that allows refraction of light entering the cornea.

Mainly, the epithelium is composed of 4-5 layers of stratified squamous epithelial cells and a single layer of basal cells. The surface area top layers (first 2-4 layers) are composed by polyhedral cells known as superficial cells or surface squamous cells; underneath these, there are 1 to 3 layers of wing cells. Instead, the latter is a single basal layer of basal cells [13]. The basement membrane is located right at the bottom of the epithelium.

Intercellular junctions of the corneal epithelium form a barrier against pathogen penetration and fluid loss. Indeed, the cells are connected by tight junctions, adherens junctions, gap junctions, and desmosomes located along the lateral epithelial cell membranes. These junctional complexes are located at different depths of the epithelium [14]. Instead, the hemidesmosome (HD) connects the basal epithelial cells to the underlying basement membrane through the integrins. Integrins are able to mediate adhesion of epithelial cells to fibronectin, collagen, laminin proteins. They have a crucial role for adhesion; when their expression decreases, cells are less adhesive to the basement membrane and less proliferative [15]. The hemidesmosome system prevents the detachment of the epithelium from the underlying layers, playing a vital role in tissue regeneration approaches. The

basement membrane is about 40 to 60um thick and mainly comprises laminin secreted by basal cells and collagen IV [16].

Furthermore, an important zone for corneal regeneration is the limbus. It is a critical and narrow zone between the conjunctiva and the cornea and represents where limbal stem cells (LSCs) reside. Renewal and repair of the epithelium surface depend on the presence of these cells. In fact, the corneal epithelium is a proliferating tissue where cells are continually renewed and replaced by a centripetal migration of LSCs from the limbal basal layer toward the corneal surface (Fig. 2). However, in the case of chemical or physical ocular burns, the limbus can be destroyed, causing the so-called limbal stem cell deficiency (LSCD), where conjunctival cells invade the corneal surface for restoring the eye [17, 18].

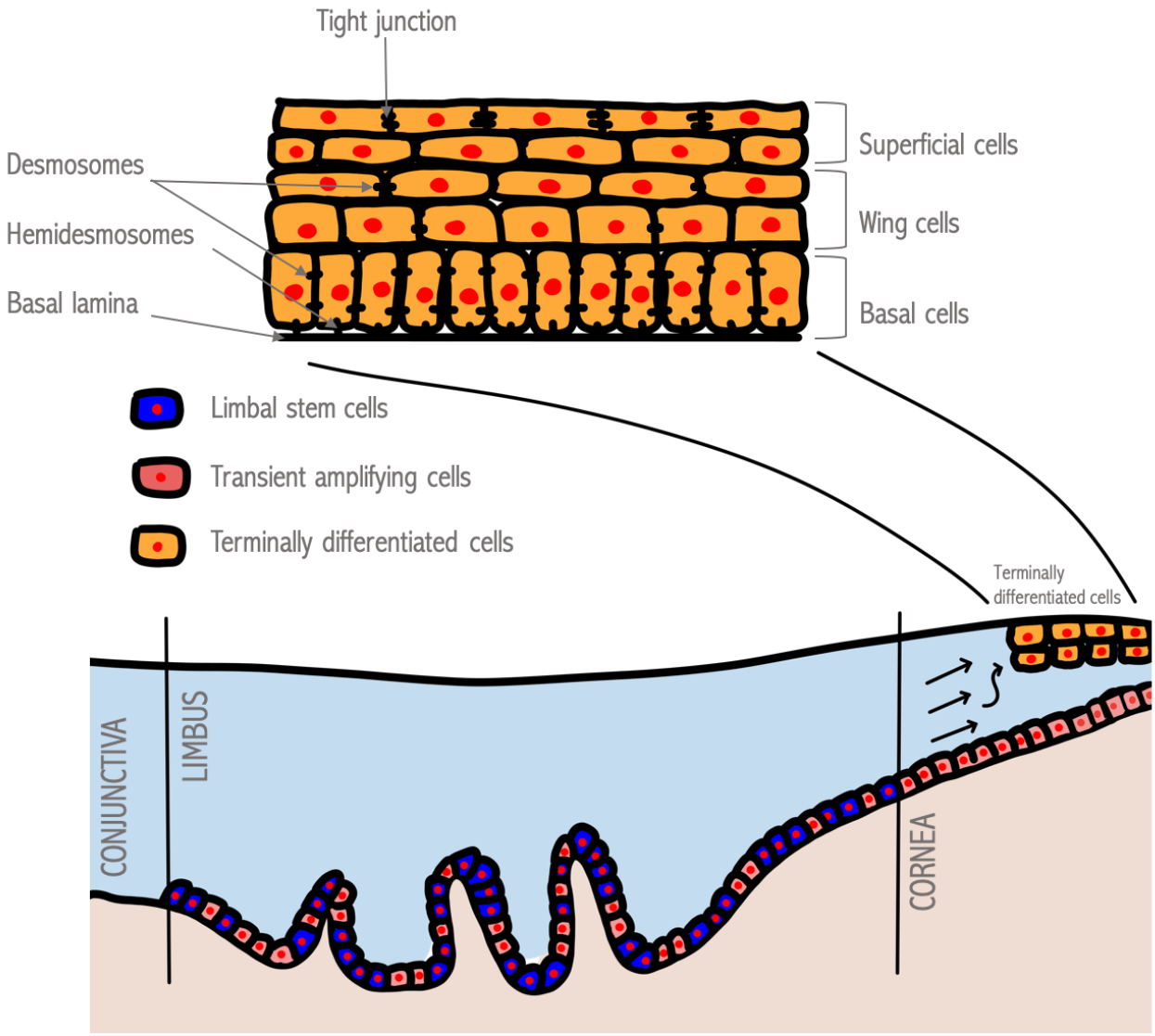

Fig. 2 Representation of the limbal niche, transient amplifying cells and epithelial terminally differentiated cells.

The clue in corneal adhesion: integrins

Integrins are transmembrane proteins that are crucial for cell adhesion and survival. They mediate the attachment of cells to substrates and they are responsible for maintaining tissue integrity, facilitating mechano-transduction between cells and the extracellular matrix (ECM) through mechanical forces. Those forces are relayed through integrin cytoplasmic domains to the cytoskeleton. In human cornea, α3β1 and αvβ5 integrins mediate adhesion through focal adhesions which are actin based, while α6β4 integrin, predominant in basal cells, mediate cell adhesion to the basal membrane via the already mentioned hemidesmosomes [15]. In fact, most integrins localize to the basal layer of cells mediating the adhesion to the ECM. The α6β4 integrin is a laminin receptor, especially it binds laminin-332 (laminin-5), that is a significant component of the epidermal basement membrane and plays a crucial role in Junctional Epidermolysis Bullosa disease [19].

The Bowman's membrane

The Bowman's membrane is an 8 to 15µm-thick acellular layer between the superficial epithelium and the stroma. It comprises amorphous, randomly oriented condensed collagen fibrils within an ECM. It acts as a link between the basal epithelial membrane and the stromal collagen lamellae. It is a condensation of proteoglycans and collagen [16, 20].

The stroma

The corneal stroma represents the 90% of the total thickness of the whole cornea. The resulting transparency of the stroma is due to the precise organization of stromal-aligned collagen fibrils and ECM. The collagen type I is predominant (13.6%) within the fibrils, together with collagen type VI and XII, as well as glycosaminoglycans (0.9%) [21]. The fibrils, made up of collagen fibers, are packed together to form lamellae (about 200-250 distinct in the whole stroma), while the collagen is found between them. The density of lamellae packing is higher in the anterior stroma compared to the posterior one. The interlacement of collagen pack between neighboring lamellae gives a significant structural substructure for shear (sliding) resistance, transferring tensile loads between lamellae [22].

The lamellae are interspersed within stromal cells called keratocytes that preserve the ECM environment and help to maintain stromal homeostasis. They synthesize collagen molecules (I, V, VI) and glycosaminoglycans, together with matrix metalloproteinases [16].

This high organization of collagen lamellae gives biophysical properties and mechanical support needed for transparency, including regular spacing, small diameter, and tight packing of collagen fibrils (fig. 3) [23].

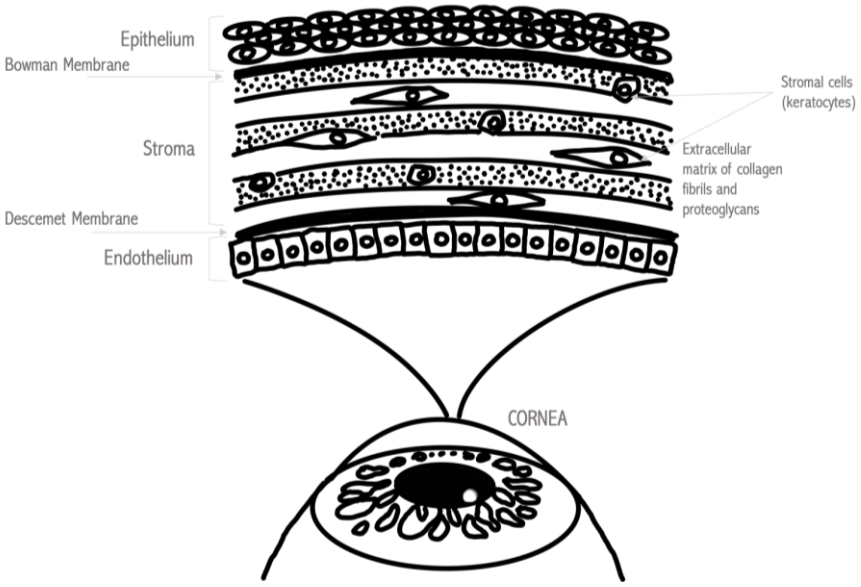

Fig. 3 Anatomy of the cornea. The stroma is the most prevalent component of the cornea. The stromal collagen layers maintain mechanical tensile resistance, and the elevated concentrations of small leucine-rich proteoglycans help regulate tissue hydration and support the inter-fibrillar spacing needed for transparency [24].

The Descemet's membrane

This membrane is 5-10µm thick, composed mainly of laminin and collagen type IV. It is secreted by endothelial cells [13].

The endothelium

The endothelium is a single layer of polygonal endothelial cells, essential for maintaining stromal hydration and transparency trough active transport mechanisms that create ion gradients to counterbalance the continuous leak of fluid into the corneal stroma [25].

The importance of the limbus for corneal regeneration

The limbal epithelium is characterized by different layers of cells organized in ridges called palisades of Vogt; it is also composed of melanocytes and Langerhans cells. As previously described, in the limbus resides the LSCs that establish renewal and repair of the corneal epithelium. Epithelial stem cells can be analyzed at a single-cell level to better understand their features. Thus, the clonal analyses of the human epithelial keratinocytes point out the presence of three different types of cells based on their growth potential; resulting in holoclones, meroclones, and paraclones presented in figure 4 [26].

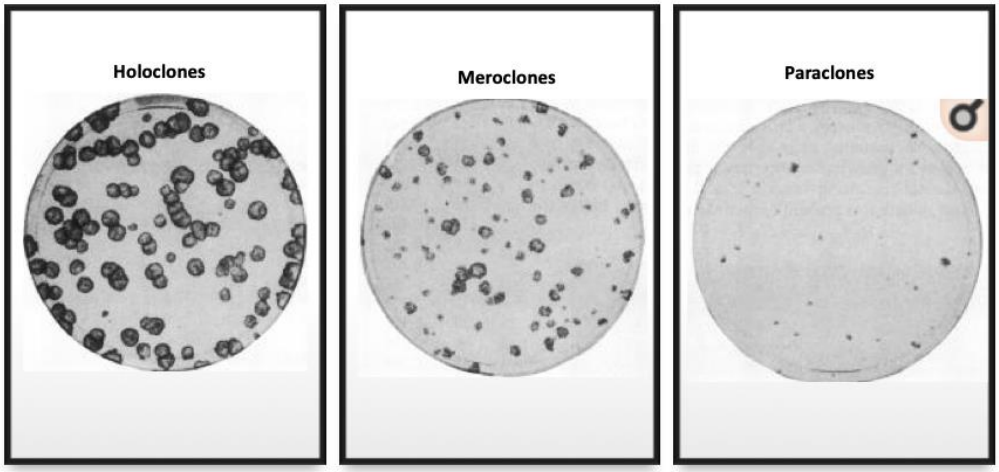

Fig. 4 Representation of the three different types of clones [26]

The holoclone-forming cell is strictly founded in the limbus; it has the highest proliferative capacity (it is able to undergo 120-160 divisions) and is the smallest colony-founding keratinocyte; considering it the epithelial stem cell [27, 28]. Holoclones have a spectacular proliferative potential: epithelial cultures maintaining holoclones-forming cells are able to permanently re-establish an extensive normal epidermis and ocular defects throughout the patient's life. Hirsch et al. in 2017 presented how autologous transgenic epidermal cell cultures with a suitable number of stem cells can replace a whole epidermis of a 7 years old Junctional Epidermolysis Bullosa patient [29].

The meroclone comprise cells with different proliferative potential, considering it as a transitional stage between holoclones and paraclones [26, 28].

The paraclone is considered a late transient amplifying cell, committed to 15 cell divisions maximum. It generates more than 95% of aborted colonies and it contains only terminally differentiated cells [26]. The passage from holoclone to meroclone to paraclone is unidirectional, and it usually occurs with natural aging or during keratinocytes sub-cultivation [28]. An important feature for identifying these clones is represented by the expression of ΔNp63. In the uninjured surface of the eye, ΔNp63α (also referred as p63α) is founded in the limbus but absent in the corneal epithelium. In fact, p63α decreases during the clonal transition from holoclone to meroclone, considering it virtually absent in the paraclones [30, 31]. When migrating, the cells that have the alpha isoform are confined to the basal layer; instead suprabasal cells contain just beta and gamma isoforms, concluding that p63α is fundamental for maintaining the proliferative potential of LSCs and their capacity to migrate over the cornea [30]. Instead, ΔNp63β and ΔNp63γ isoforms take part in epithelial differentiation, precisely during the process of corneal regeneration [18, 32].

Thus, the corneal surface can be successfully repaired and renewed by LSCs. The depletion of the LSCs causes severe to total LSCD, and this can result in a process called conjunctivalization, in which neovascularization, chronic inflammation, corneal opacity, and in some cases, complete visual loss occurs due to bulbar conjunctival cells invading the corneal surface trying to restore the epithelium [17]. Thus, the only strategy that prevents this cell invasion is to restore a normal limbal/corneal

epithelium. To date, the main primary treatment for LSCD is represented by Holoclar®, the first Cultured epithelial transplantation procedure for the treatment of visual impairment and blindness. Holoclar® is the first stem cell-based medicine approved by the European Medicines Agency (EMA) in 2015 [33] that is able to replace epithelial cells in a damaged cornea and to permanently restore a functional, healthy corneal epithelium allowing recovery of complete visual acuity [34]. The use of a small limbal biopsy (1–2 mm^2) containing autologous LSCs represents the innovation of Holoclar® as a treatment. The LSCs extracted from this biopsy are expanded in a GMP-approved laboratory (good manufacturing practice-approved laboratory) to repair the damaged corneal surface when seeded onto a fibrin matrix. In particular, LSCs are cultivated on a GMP-certified lethally irradiated feeder layer (F/L) of 3T3-J2 cells as previously described by Rheinwald and Green in 1975 [3, 35-37]. The clinical success of this therapy is directly correlated with a certain amount of stem cells present in the limbal cell culture. The stem cells, as previously described, can be identified through their specific dimensional range and high-level expression of ΔNp63α positive cells [30].

Despite the clinical success, Holoclar® is not sufficient in case of deeper severe damage that comprises the stroma. For this reason, the development of a TE product composed of autologous LSCs which can properly grow onto a transparent scaffold as a substitute for the corneal stroma, could represent a new alternative to corneal transplant for patients with LSCD and stromal scarring.

In fact, within corneal regeneration, the Advance Therapy Medicinal Product (ATMP) Holoclar® has been successfully approved and used in clinical applications for the restoration of corneal epithelium. In contrast, the *in vitro* reconstruction of corneal stroma and the growth of *in vitro* cultured endothelial cells still represent a challenge; even if several attempts have been described [38].

Thus, in the presence of significant stromal damage, TE stromal approaches represent the forefront of the innovation and the personalized medicine functional to substitute one of the most used techniques to restore visual acuity: the penetrating keratoplasty (PK) procedure. This approach is represented by a corneal transplantation with a full-thickness human donor cornea graft and it should be overcome due to the significant complications of immunological rejection, glaucoma, and microbial keratitis, which continue to limit success [39].

Therefore, a range of TE approaches is being evaluated worldwide as substitutes for keratoplasty procedure that constantly represents the so-called traditional therapies. These invasive surgical options can be costly for the society and non-definitive on long-term [2].

Tissue Engineering in corneal regeneration

The TE is an interdisciplinary field of research that includes the fundamentals of engineering, materials science, medical research and life sciences. It intends to substitute an entire organ or allow the restoration of the selected cellular functions [40].

The relation between corneal restoration and quality of life is described in the literature [41, 42]. A global corneal transplantation survey reported a significant lack of donor corneas used for penetrating keratoplasty procedure, with a ratio of 1:70 cornea available for patients in all the world [43].

In addition to restoring sight, a corneal TE transplant can avoid higher medical costs, the opportunity cost of lost productivity, and potential long-term care cost, all by eliminating blindness or significant visual impairment. It is estimated that an average person whose vision has been restored through a corneal transplant procedure will avoid about $214,000 in indirect costs over the course of patient life [2, 44]. Also, due to the increasing number of transmissible disease and the aging of the population, the need for alternative corneas will continue to grow. Applying new TE approaches in everyday lives will further improve the quality of life thanks to increased biocompatibility and longer duration of implants; also, patients won't need immunosuppression and could resume their everyday life. Innovative biomaterials will supply novel patient-tailored corneal scaffolds as a solution for tissue regeneration without the need for insufficient cadaveric donor tissues and with reduced risks of disease transmission and immunologic reactions for better, safer, and personalized healthcare (Table 1) [45].

Various principles have been used in the development of viable cornea tissue equivalents. The goal is to generate full-thickness corneal tissue constructs made up of several biomaterial systems to generate TE at various levels of complexity, starting from engineering the three cellular layers, up to nerve innervation approaches.

Design process	Application to cornea
Define problem 	A lack in full-thickness or hemi- corneal autologous substitutes
Define requirement for the user 	For the patient: to restore visual acuity without complications and pain For the surgeon: easy approach to handle, standardization For the Society: reduced costs, market scale
Specify material requirement 	Biocompatibility, biodegradability, significant biomechanical strength and high transparency
 Design prototype of the material	Select the ideal material, fabrication steps, sterilization techniques etc.
Evaluate and optimize the cell-material product 	*In vitro*: characterization of the cells type used; physical and mechanical tests on the material

Table 1. The process design to develop corneal scaffolds

The scaffold represents the microenvironment for cell proliferation and survival, and it constitutes the basis for cornea regeneration and its biological characteristics. An ideal scaffold should be (i) a temporary support, being the contour for corneal repairing, (ii) a carrier for adhesion, proliferation, migration, and differentiation of corneal cells, guiding the growth of seeded cells [46]. Especially, biomaterials needed for TE corneal substitutes (iii) should replicate the functional and structural requirements of the native cornea.

Nowadays, different scaffold materials for corneal replacement have been proposed; divided as natural materials and synthetic polymers. Natural polymers have excellent biocompatibility. Instead, synthetic polymers can be customized to obtain the desired properties (Table 3) [45].

Natural materials

Natural biomaterials have excellent biocompatibility compared to synthetic polymers. They are able to mimic the mechanical and biological function of the natural ECM *in vivo*. These biomaterials can be classified in protein-based materials (gelatin, collagen, silk etc.) and polysaccharide based material (chitin/chitosan, cellulose etc.).

Collagen

The collagen is the principle structural protein of most tissues and represents about 71% of the dry weight of the healthy donor stroma. It embodies an ideal candidate for TE approaches since it is the main component of ECM in most tissues, maintaining its structural and biological integrity and delivering physical support to tissues and cells.

There are about 29 known collagen isoforms described worldwide. It can be purified on a full scale and it is easy to isolate. Also, its structural, immunological, chemical and physical properties are very well documented. Finally, thanks to its non-cytotoxic, biocompatible and biodegradable properties represent an easy biomaterial for tissue regeneration approaches [40].

Especially Collagen type I represents the most used in 3D reconstruction because it's of easy production and cheap to derive. Pre-clinical studies on cell-free corneal ECM mimics, realized by the use of recombinant human collagen (RHC), were sufficient for corneal regeneration in animal models [5, 39].

Gelatin

The gelatin is a natural protein that derives from the hydrolysis of collagen. It is used in different TE applications including the cornea. It is widely considered due to its properties such as its biocompatibility, low cost, and low immunogenicity. However, gelatin lacks thermal stability and undergoes degradation quickly unless chemically crosslinked or combined with another material [45].

Fibrin

Fibrin is a blood coagulation factor, and it can be used as a sealant. It is usually made by fibrinogen that completes the final step of natural coagulation with thrombin. It is a biodegradable tissue adhesive that can be entirely degraded *in vivo*. Rama et al. presented impressive cultivation of limbal cells on fibrin that was placed onto a plastic ring, finding it as a highly manageable and fast degradable natural substrate [47].

Amniotic membrane (AM)

It is the innermost layer of the placenta and both fresh and preserved AM are investigated as a substitute for the ocular surface [48]. For decades, it has been used as a substrate for LSCs cultivation and transplantation because of its proven effectiveness in promoting epithelialization, reducing scarring, inflammation, and angiogenesis. In fact, in 2000, Tsai et al. showed some results in growing limbal epithelial cells on AM support using it as a matrix for cell growth and migration [49]. However, the possibility of infection and the short tissue source led to the research of new safer alternatives.

Hyaluronic Acid (HA)

The HA is one of the profuse polysaccharides in the human body, composed by repeated disaccharide units of N-acetyl-d-glucosamine and d-glucuronic acid. Due to its chemical properties (the solubility and the accessibility of the refractive functional groups) it is considered a great option in case chemical modifications are needed and for TE approaches due to its biocompatibility [40]. Both *in vivo* and *in vitro* studies point out the ability of HA to stimulate wound healing [50]. In fact, it can up-regulate the expression of anti-inflammatory cytokines related to tissue healing and repair and, on the contrary, down-regulate the expression of inflammatory cytokines [51]. However, several more attempts must be done, since in corneal ulcers it is still not sufficient to accelerate the wound healing process [52].

Silk Fibroin (SF)

Silk Fibroin is a natural structural protein derived from the cocoon of the silkworm *bombyx mori*. It has been extensively used in TE approaches thanks to flexibility, controllable degradation rates, non-immunogenic response, and mechanical properties such as high tensile strength. Also, its inherent optical clarity can be considered a good candidate in corneal engineering approaches [53]. The SF can be easily incorporated in various materials for biomedical applications such as enzyme immobilization matrices, drug delivery carriers, and scaffolds that can replace connective tissue and promote cell growth [54]. The SF fiber has also been used as a suture surgical material, frequently used in corneal tissue engineering.

Chitin and chitosan

The chitin is the second copious natural biopolymer after cellulose, and it can be easily found in exoskeletons of insects, crustaceans, and fungi cell walls. Chitin is a high molecular weight, non-toxic and linear biopolymer. It is a polysaccharide, structurally N-acetyl-D-glucosamine (N-acetyl-2-amino-

2-deoxy- D-glucopyranose) units linked through β-D (1 → 4) bonds stretching [55]. Chitin can be found crystallized into three allomorphs that are respectively α, ß, and γ forms. α-Chitin is the most common and stable form; it is present in different living organisms such as yeast and fungal cell walls, lobster, crab tendons and shells, insect cuticle, etc. It packs in antiparallel molecular chains. Instead, β-chitin is present in tubeworms and squid pens and is made of parallel molecular chains. The γ form is less known and is considered a variant of α-chitin (Fig. 5) [56].

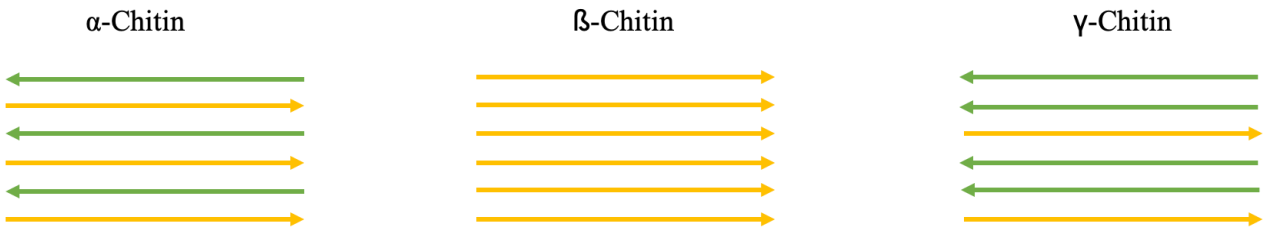

Fig. 5 The three polymorphs of chitin have different chitin chains orientation.

The chitosan is a partially deacetylated product of the chitin and its most derivative. It is obtained by a deacetylation reaction (free amino groups left by partial removal of acetyl groups of chitin) [54, 55].

Chitin-based materials are preferred over other natural materials due to their biocompatibility, non-toxicity, biodegradability, and bactericidal effect. The positive charge of the amino group can react with anions present on the bacteria cell wall [57].

Synthetic polymers

Synthetic polymers are a class of three-dimensional macromolecular polymer networks obtained from physical and/or chemical cross-linking, which have high hydrophilicity but are insoluble in water. Their ability, compared to natural materials, is to provide significant control over the property adjustment or the characteristics of the materials.

Thermal responsive polymers: Poly(N-isopropylacrylamide) (PNiPAAm)

These polymers have been widely used in TE approaches and are considered one of the essential thermo-responsive polymers due to their hydrophobic and hydrophilic properties; this is helpful for cell sheet detachment without using enzymatic digestion. This synthetic polymer material has different sources, controllable mechanical properties, and a simple manufacturing process.

Thus, its main characteristic is the thermo-reversible gelation properties into aqueous solutions. This material can gel when 32-35°C is reached and turn into a solution upon cooling [58]. The hydrophobic/hydrophilic state can be changed, varying the temperature above or below a critical value, known as the lower critical solution temperature; which, for this material, is close to body temperature (36.5-37.5°C) [59].

Other synthetic polymers hydrogels: PGA, PLGA and PEG-DA

The polymer materials of polyglycolic acid (PGA), and poly(lactic-co-glycolic) acid (PLGA) are considered a good option for biodegradable and biocompatible medical implants for TE purposes, for drug carrier designs and even as a use in the packaging industry [60]. However, PGA network fibers are unable of resisting substantial compressional forces; thus, due to their fast degradation PGA-based scaffolds are more used for sutures fabrication and as a drug delivery carriers [61]. Another common used synthetic polymer is the polyethylene (glycol) Diacrylate (PEGDA). All of these materials present a great permeability, good optical and mechanical properties; however, they exhibit poor cell-adhesive function when not modified on the surface. For example, to improve cell attachment and growth of primary human and rabbit corneal cells, PEGDA hydrogels were modified with RGD, phosphate groups and collagen type I [62].

3D bioprinting for corneal TE approach

The 3D bioprinting represent a novel technology that can be used to fabricate biological tissue for TE and clinical applications. The aim is to manufacture a scaffold that resemble the structure of the natural human corneal stroma [63]. It is considered a novel technology because of the possibility to made a layer-by-layer deposition of biological material, reproducing the anatomy and structure of a native corneal stroma [64] with its biomechanical functional and structural properties [65], in a short time frame. There are three major 3D printing techniques that can be subdivided in droplet-based, extrusion-based and laser-based approaches (Table 2) [66].

The extrusion-based printing is the commonly used. It is characterized by extruding fine filaments of pre-polymerized bioinks that comprises the use of a needle, into a printing platform through the application of pressurized air to the head of the printer. It can have more than one printer head and it can be replicated layer by layer up to the generation of the 3D construct. The plus of this method is its compatibility and that it comprises an extensive range of injectable hydrogels commonly used for applications in regenerative medicine [67]. Instead, droplet-based bioprinting is a type of inject bioprinting based on bio-ink droplets deposition. The laser-based approach comprises a laser stimulation. The final choice on the most suitable method depends on the specific application needed since each technique has its own characteristics resulting in different outcomes [66].

In conclusion, the 3D bioprinting could be a great option for artificial corneal reconstruction. However, it is still indispensable to improve this technology and the starting materials used, as well as to improve the printing equipment.

3D printing techniques	 Extrusion based	 Droplet-based (inkjet)	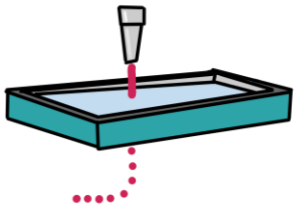 Laser-based
Mode of use	It uses mechanical force to deposit a continuous flow of bio-ink	Inkjet bioprinting, based on deposition of bio-ink droplets	Laser-assisted bioprinting, based on laser stimulation
Activator	Pressure	Temperature / voltage	Laser
Structural integrity	High	Low	Low
Print speed	Slow	Fast	Medium
Resolution	Moderate (about 200 µm)	High (0.5 – 50 µm)	High (about 1 µm)
Cell viability	45 - 98%	70 - 90%	>95%
Cost	Medium	Low	High

Table 2. The three different 3D printing methods and their features

Functionalization of biomaterials to improve cell attachment and proliferation

Biomaterials can also be improved using ECM molecules to improve cell proliferation and migration. These molecules are added to support biological functions, as a biomechanical support and among all, to establish the correct 3D environment mandatory for cell attachment and proliferation. Each protein has a distinct impact on cell behavior and growth, thus, these proteins used in regenerative medicine approaches help to functionalize the material [68]. In figure 6 there is an overview of the main molecules involved in the process of cell attachment.

To improve biomaterials, a protein or a combination of proteins can be chosen depending on the desired effect or the target application. These proteins can be either be isolated by animal or human tissues [69] or be artificial; the so-called artificial or ECM-like proteins that can be comparable to full-

length proteins and be synthetically generated. They can contain a certain molecular weight and have a defined sequence [68].

Especially, the coating procedure represent a modification of the surface and has an important role in TE and applications in regenerative medicine. They can potentially improve biocompatibility and enhance cell adhesion [70]. Thus, the easiest way to bind ECM molecules to the surface of a substrate is the coating procedure that involves a non-specific physical adsorption on a surface. Jia et al. in 2015 presented an RGD modified silk films together with a poly-D-lysine coated silk films applied to TE and corneal regeneration. The group proved that adding the RGD to the poly-D-lysine increased the viability and the proliferation of human corneal epithelial cells [71].

Another example, talking about the increase of cell adhesion, are the aptamers. Aptamers are a single strand DNA (ssDNA) or RNA (ssRNA) oligonucleotides with a length from 20 to 100 nucleotides and thanks to their specificity and selectivity they are able to bind small molecules (peptides, proteins, vitamins, metal ions, particles and even whole cells). The interesting ability is that they (i) are extremely specific to their targets molecules and simply conjugated to different ions and surfaces (ii) are smaller than antibodies (iii) can be modified post-production [72]. They have been already widely used for cancer, age-related macular degeneration, inflammatory diseases and thrombosis.

Aptamers can be obtained from nucleic acid libraries and developed using the systematic evolution of ligands by exponential enrichment technology (SELEX) selection process. This technique requires simple separation steps of DNA or RNA that identify target molecules from the DNA or RNA libraries. These steps are repeated until the selection leads to the isolation of the high affinity aptamer [73].

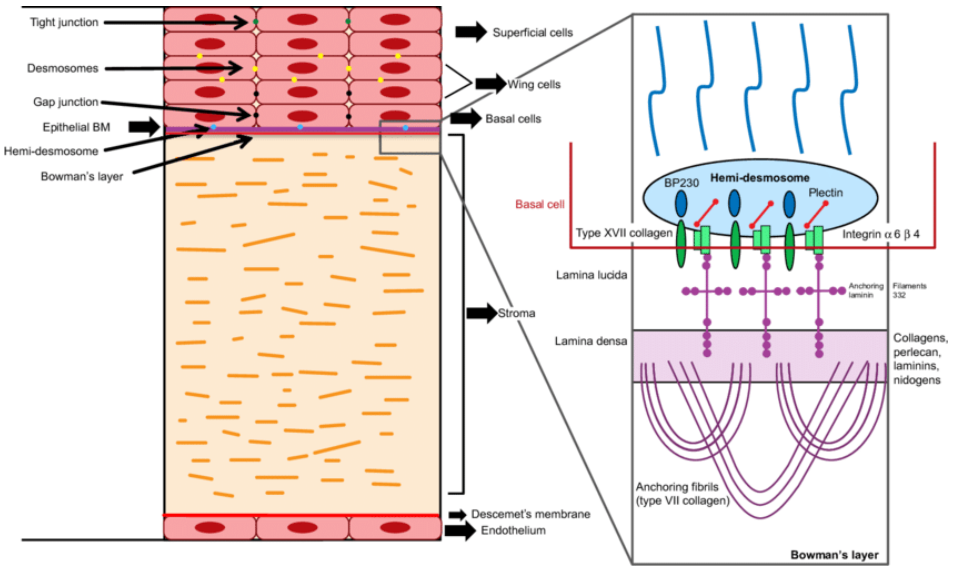

Fig. 6 The adhesion complex [74]. The complex between the epithelium and the basement membrane is crucial for epithelial adhesion, and proliferation. Different proteins, including hemi-desmosomes complex, collagen types IV, VII, and XVII, and MMPs, regulate its adhesion and modulate the wound healing process.

Epithelium and stroma		
Scaffold material	Tested *in vivo*	Reference
Porcine collagen I	Rabbit	*M. Koulikovska et al. Tissue Eng., Part A 2015 & M. Rafat et al. Biomaterials 2016*
Rat collagen I	Rabbit	*N. Builles et al. Biomaterials 2010*
Bovine collagen I	Rabbit	*Y. Liu et al. Int. J. Biol. Macromol. 2019*
Bovine collagen I	Dog	*E. Bentley et al. Cornea 2010*
Bombyx mori	No	*L. J. Bray et al. Biomaterials 2012 & S. Wang et al. Biomaterials 2017 & E. A. Gosselin et al. Tissue Eng. Regener. Med. 2018*
Antheraea mylitta	Rabbit	*S. Hazra et al. Sci. Rep.* 2016
Bombyx mori and chitosan	Rabbit	*L. Guan et al. Cells Tissues Organs 2013*
Bombyx mori and collagen	Rabbit	*K. Long, Y. Liu et al. Biomed. Mater. Res., Part A 2015*
GelMA	Rabbit	*E. S. Sani et al. Sci. Adv. 2019*
Hyaluronic acid	No	*L. Koivusalo et al. Biomaterials 2019 & L. Koivusalo et al. Mater. Sci. Eng., C 2018*
Fibrin + agarose	Human	*L. Rico-Sanchez et al. J. Tissue Eng. Regener. Med. 2019 & M. Gonzalez-Andrades et al. BMJ Open 2017*

Stroma only		
Scaffold material	Tested *in vivo*	Reference
Rat collagen I	No	*M. Ahearne et al. Tissue Eng., Part C 2010 & M. Ahearne et al. Exp. Eye Res. 2010 & C. Kilic et al. Biomater. Sci. 2014*
Rat collagen I	Rabbit	*X. Xiao et al. J. Biomed. Mater. Res., Part A 2014*
Rat collagen I + PA	No	*M. Miotto et al. Adv. Funct. Mater. 2019*
Bovine collagen I	No	*M. L. Borene et al. Biomed. Eng. 2004 & E. J. Orwin et al. Biomech. Eng. 2003 & V. Kishore et al. Biomed. Mater. 2016 & R. A. Crabb et al. Ann. Biomed. Eng. 2006*
Bovine collagen I	Pig	*F. Li et al. Biomaterials 2005*
Porcine collagen I	Guinea pig	*C. R. McLaughlin et al. Biomaterials 2010*
Recombinant human collagen I and III	Mini-pig	*K. Merrett et al. Invest. Ophthalmol. Visual Sci. 2008*
Recombinant human collagen III	No	*S. Hayes et al. Acta Biomater. 2015*
Recombinant human collagen III	Human	*P. Fagerholm et al. Biomaterials 2014 & P. Fagerholm et al. Sci. Transl. Med. 2010 & P. Fagerholm et al. Clin. Transl. Sci. 2009 & O. Buznyk et al. Clin. Transl. Sci. 2015,*
Bombyx mori	No	*B. D. Lawrence et al. Biomaterials 2009 & E. S. Gil. et al. Macromol. Biosci. 2010 & M. C. Lee et al. Biomed. Mater. Res., Part B 2016 & W. Zhang et al. Adv. Healthcare Mater. 2017 & C. E. Ghezzi et al. PLoS One 2017*
Bombyx mori	Rabbit	*C. E. Ghezzi et al. Appl. Biomater. Funct. Mater. 2016*

Bombyx mori and RGD peptides	No	*E. S. Gil et al. Biomaterials 2010 & J. Wu, J. Rnjak-Kovacina et al. Biomaterials 2014*
Bombyx mori and chitosan	Rabbit	*L. N. Guan et al. Mol. Histol. 2013*
Bombyx mori and RGD peptides	Rabbit	*L. Wang et al. Biomed. Mater. Res., Part B 2015*
Bombyx mori, retinoic acid, and riboflavin	No	*P. Bhattacharjee et al. Mater. Sci. Eng., C 2019*
Gelatin	Rabbit	*T. Mimura et al. Mol. Vision 2008 & L.-J. Luo et al. Acta Biomater. 2018*
Gelatin + GAG	Rabbit	*J. Y. Lai, et al. Int. J. Nanomed. 2012 & J. Y. Lai et al. Int. J. Mol. Sci. 2013*
Gelatin + collagen I	No	*H. Goodarzi et al. Int. J. Biol. Macromol. 2019*
GelMA	No	*C. K. Bektas et al. Tissue Eng. Regener. Med. 2018*
Fibrin + fibronectin	No	*M. Miron-Mendoza et al. Matrix Biol. 2017*
Alginate	No	*K. Tonsomboon et al. Behav. Biomed. Mater. 2013*
Magnetically aligned rat-tail type I	No	*Torbet J et al. Con Proc IEEE Eng Med Biol Soc 2007*
Polyglycolic acid fibers	No	*Hu X.J. Et al. Tissue Eng 11, 1710, 2005*

Table 3 Summary of different scaffolds used for epithelial and stromal replacement and stromal replacement only.

Materials and Methods

Chitin scaffold from squid pen

The chitin scaffold should be functionalized with some molecules to let properly attach the keratinocytes to the biomaterial. Specifically, this material derives from *Loligo Vulgaris* squid pen. It is of natural origin, transparent, biocompatible and biodegradable (Fig. 7).

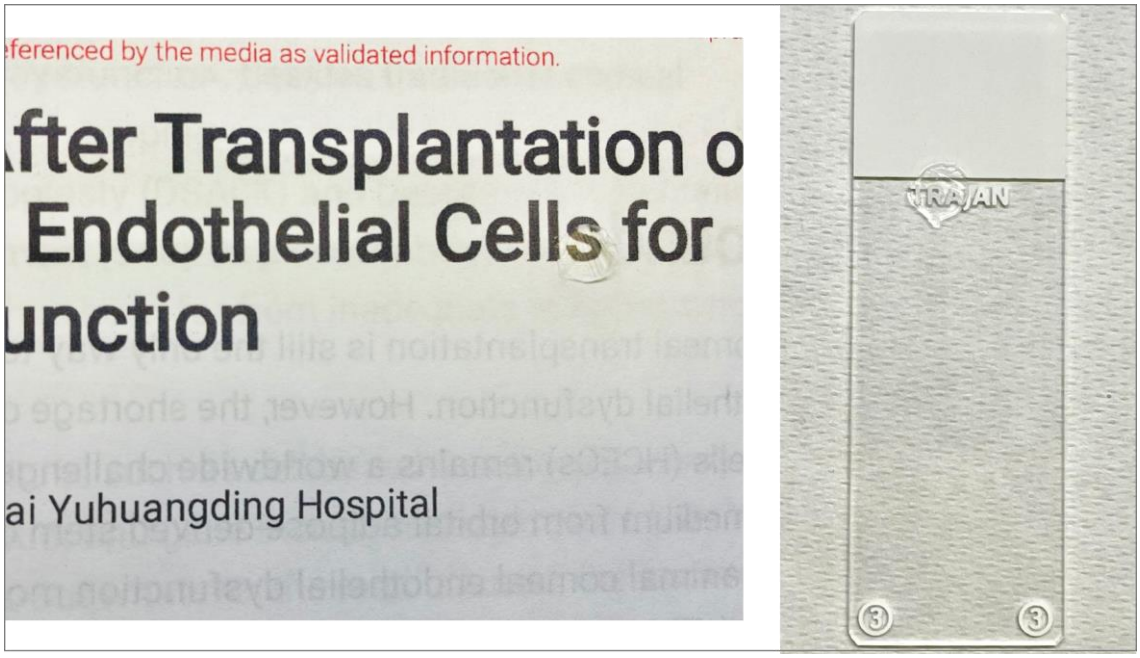

Fig. 7 Pictures highlighting the transparence of *Loligo Vulgaris* squid pen

Chitin scaffold pre-treatment: deproteinization step

The selected scaffold was deproteinized by sterile fresh 1M NaOH solution for 2 hours at 100 °C on stirring. Then, the scaffold was cleaned with Mili-Q water over-night (O/N) at 4°C. After the deproteinization step, the material was sterilized by high pressure saturated steam (autoclave) at 121°C for around 20 minutes. To perform this step, the material was put in a 50 ml tube with phosphate-buffered saline (PBS) 1x.

Chitin scaffold pre-treatment: functionalization step

To perform the scaffold functionalization; different options were performed, based on different experiments carried out (Fig. 8):

Condition A) Human Fibronectin and Collagen IV: 60 µg/ml of human placental collagen IV (Sigma-Aldrich, cat. no. C5533) was mixed with 20 µg/ml of human fibronectin (Corning Life Sciences, cat. no. 354008) and placed onto the selected chitin scaffold. Collagen IV and fibronectin were incubated for 1 hour at room temperature (RT). After incubation, the scaffold was rinsed three times with sterile PBS 1x to remove all traces of free collagen and fibronectin. Thus, the treated scaffold was let it dry for 1 hour at RT and then sterilized with UV light for another hour in dry conditions. After these steps,

the scaffold was rehydrated with PBS 1x and was used for F/L cells seeding and then, keratinocyte cells seeding as described.

Condition B) Aptamer anti-laminin: customized ssDNA aptamers screened against human laminin (ATW0024, Base Pair Biotechnologies, Pearland, TX) and modified with a short carbon chain containing a disulphide bond on their 3′ end and with a biotin on their 5′- end, were used. Anti-laminin aptamers were 40 nucleotides long and 12597.4 g/mol heavy.

Deproteinized and sterilized chitin scaffolds were functionalized with 20 µg/ml of the aptamer anti-laminin for 1 hour at RT. Then, exogenous LN332 or LN511 laminin (Human recombinant laminin 511 and Human recombinant laminin 332, BioLamina) were first re-suspended following the BioLamina protocol and then 5 µg/ml, 10 µg/ml and 15 µg/ml were incubated with the scaffolds O/N at 37°C. The next day, depending on the experiment, the scaffolds were rinsed and F/L and keratinocyte cell types were seeded or just keratinocytes were seeded and cultured as explained (Condition B1, Figure 8).

In another condition tested, after adding the aptamer anti-laminin to the scaffold, the material was functionalized with endogenous laminin produced by the same keratinocyte. Keratinocytes were seeded in high density (15.000 cells/96w dimension) to obtain a natural laminin coating. F/L and keratinocyte cell types were seeded and cultured as previously explained (Condition B2, Figure 8).

Condition C) Aptamer anti-fibronectin: customized ssDNA aptamers screened against human and bovine fibronectin (ATW008, Base Pair Biotechnologies, Pearland, TX), and modified with a short carbon chain containing a disulphide bond on their 3′ end and with a biotin on their 5′- end, were used. Anti-fibronectin aptamers were 40 nucleotides long and 12597.4 g/mol heavy. The presence of aptamers on the scaffold was confirmed using a cyanine blue light-fluorescence DNA intercalating dye (SYBR-Safe DNA gel stain, Life Technologies).

Chitin scaffolds were first deproteinized by sterile fresh 1M NaOH solution for 2h at 100 °C on stirring and sterilized in autoclave as explained before, then the sterilized scaffolds were functionalized with the aptamer anti-fibronectin following the Base Pair Biotechnologies protocol (Base Pair Biotechnologies, Pearland, TX). The following day, the functionalized scaffolds were coated with 20 µg/ml of human fibronectin (Corning Life Sciences, cat. no. 354008) for 1 hour at RT, then some conditions were dried in air for 1 hour (Condition C2, Figure 8), others were kept in a PBS 1x solution (Condition C1, Figure 8) for 1 hour. The process of aptamer adsorption on chitin and its release were monitored by spectrophotometry (Nanophotometer, Implen GmbH) measuring the absorbance at 260 nm. Then, F/L cells and keratinocyte cells were seeded as explained.

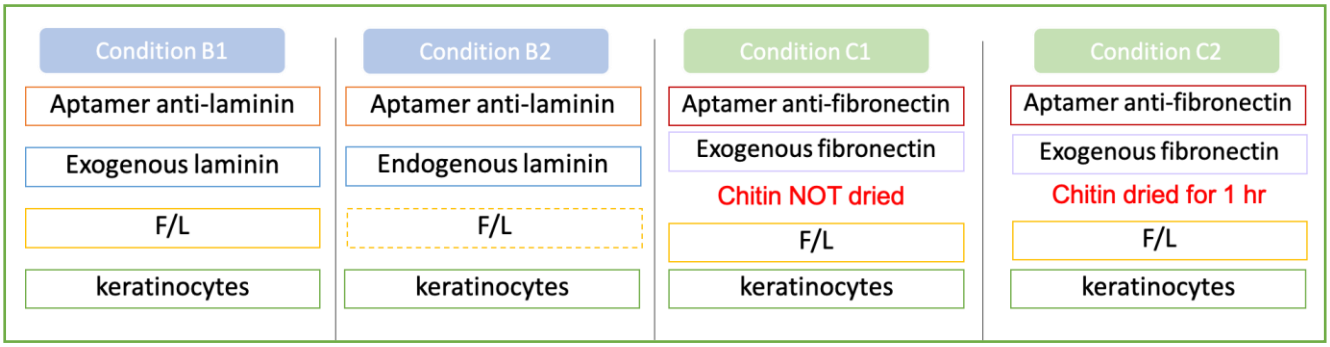

Fig. 8 Different conditions tried with aptamers. Condition on plastic (with F/L cell seeding and keratinocyte cell seeding) was performed as a control condition.

Dimethylacetamide (DMAA) - lithium chloride (LiCl) film and Acetic Acid (AcOH) film

The following steps have been realized in collaboration with the Chemistry Department "Giacomo Ciamician" of the University of Bologna, Italy.

β-chitin purification from squid pens

Squid pens from *Loligo vulgaris* were collected from a local market. Once hydrated, the lateral blades were isolated, cleaned with distilled water and ethanol 70 vol.%, and then stored dry.

The β-chitin was purified from the squid pens by alkaline deproteination. The protocol included 2.5g of washed squid pens in 100 mL of a boiling 1 M NaOH solution, and stirring for 1 hour. After that, the solution was changed with a fresh 1 M NaOH solution and refluxed for another 1 hour. The obtained chitin films were washed at RT first with a 1 M NaOH solution and then with distilled water until the washing solution had neutral pH. The chitin films were stored dry in a desiccator.

Preparation of the DMAA and LiCl film

The chitin films were obtained by dispersing 0.3 wt.% of β-chitin in a dimethylacetamide and lithium chloride (5 wt.%) solution and stirring for 24 hours. The solution obtained was then filtered on a 0.5 mm mesh filter to eliminate any aggregate. Aside, 0.5 mL of collagen in DMAA/LiCl were prepared adding a 20 µL aliquot, composed of acetic acid solution 0.5 M and 10 mg/mL of collagen in acetic acid 0.5 M in different ratios (2:0, 1:1, 0:2), to 0.48 mL of DMAA/LiCl solvent. Subsequently, 4 mL of chitin solution were placed in a beaker and the 0.5 mL of collagen solution was added dropwise under vigorous stirring. The chitin was then precipitated by exposing the solution to an atmosphere saturated with water vapors at 25°C for 24 hours.

At the end of the assembly, a gel was obtained. This gel was air dried by eliminating the solvent by mechanical pressure between paper towels. The film obtained was then washed by immersing it twice in acetone for 30 minutes each time, then twice in ethanol for 30 minutes, and lastly in water O/N. Finally, the film was dried between two glass slides to flatten it.

These films are composed of α-chitin and collagen IV. To sum up, they were obtained by dispersing the α-chitin and collagen in DMAA and LiCl and then reassembling it by slow diffusion of water.

The DMAA is a widely used as strong polar aprotic solvent. However, exposure to DMAA must be controlled due to its cytotoxic effects.

Preparation of the AcOH film

A 1 mg / mL β-chitin dispersion in AcOH at pH 3 was obtained by two different methods:

- Magnetic stirring for 72 h

- Using a blender for 6 minutes

The gel obtained was concentrated at 10 mg /mL by lyophilizing the gel and dispersing the lyophilizate in a smaller solvent volume. As for the previous method, an aliquot of 10 mg/mL collagen solution in acetic acid 0.5 M was added to the gel to obtain the desired collagen concentration. The film was then prepared by drying several gel volumes in an oven at 37°C. These films are composed of only β-chitin and collagen IV.

Also, four samples were examined:

- two obtained by depositing 0.4 mL of each of the two dispersions obtained in a 24-well plates,

- two by depositing 0.7 and 1.0 mL of the dispersion obtained by blender.

The first two samples were examined to evaluate the chitin obtained by the two methods, the other samples to define the influence of the film thickness. The films were then hydrated and their absorption spectrum in water and swelling was measured.

Functionalization of DMAA/LiCl and AcOH films

The chitin films obtained from DMAA/LiCl and AcOH were preserved in parafilm-sealed Petri dishes at 4 °C. Then, two quick washes in distilled water (ddH_2O) were performed to re-hydrate the samples.

Subsequently, UV rays for 1 hour were performed to sterilize the materials. Then, the scaffolds were coated with Laminin 5 (LN332, Biolamina) at a concentration of 5ug/mL on all conditions (including control conditions without collagen IV) O/N at 4°C in sterile multiwall. The next day, the chitins were moved in a new well, washed with ddH_2O, and the F/L was seeded onto the scaffolds. The keratinocytes were seeded and cultured after 2-24 hours, as explained.

Chitin scaffold with RGD peptide

The following steps have been realized in collaboration with the Chemistry Department “Giacomo Ciamician” of the University of Bologna, Italy. The chitin scaffolds used are deproteinized squid pen (with a degree of acetylation around 75%) on which a decapeptide (containing the RGD sequence) was linked to the free amine groups of chitin.

Preparation of chitin matrix

After the initial deproteinization described at in "β-chitin purification from squid pens" a second more aggressive alkaline treatment was performed to further deacetylate the chitin. About 1 g of chitin was placed in 50 mL of boiling 5 M NaOH. The chitin was then boiled under reflux for two hours under mild magnetic stirring. In the end, it was washed several times with distilled water until the neutral pH of the washing water was reached. The chitin obtained was then dried in a dryer. This treatment produces chitin with a degree of deacetylation of 23.1%.

Chitin-peptide coupling

The chitin was hydrated in a 9:1 dimethyl sulfoxide/ 0.1 M phosphate buffer solution at pH 7.4 for 30 minutes. Then, two solutions were prepared using the same buffer: (1) a 16.24 mg/ml peptide solution and (2) a solution containing EDC ((1-ethyl-3-(3-dimethyl aminopropyl) carbodiimide) and NHS (*N*-hydroxysuccinimide) with a concentration of 2.8 mg/ml and 1.68 mg/ml, respectively. These two solutions were mixed and slowly dripped onto the chitin solution. The mixture was left under stirring with a magnetic stir bar at room temperature for 18 hours. The chitin was, finally, washed twice with dimethyl sulfoxide, acetone and ethanol, three times with water and dried in a dryer. Finally, the UV spectra of the chitin were acquired.

Chitin post coupling characterization

To determine wheteher the lamellar structure of the chitin was preserved during the coupling reaction, X-ray diffractograms, FTIR spectra, optical microscope, and scanning electron microscope (SEM) images were acquired.

Furthermore, the swelling values and the thickness of the chitin fragments were determined. To evaluate the chitin swelling, the samples were weighed after being soaked in water overnight, prior blotting on a paper tissue, then dried in a desiccator overnight and finally weighted again. The swelling was calculated as a percentage of the ratio between the hydrated and dry state.

Squid pen coated with lectins and RGD sequence

The following steps have been realized in collaboration with the Chemistry Department "Giacomo Ciamician" of the University of Bologna, Italy. Those steps include tests of binding of the RGD peptide to the squid pen by means of lectins.

In literature, there are many lectins of plant origin that are able to selectively bind chitin. In fact, lectins have a role in recognition on the cellular and molecular level and play numerous roles in biological recognition phenomena involving cells, carbohydrates, and proteins.

Chitin-peptide lectin coating

A deproteinized squid pen fragment, cut into a square of side 5 mm (dry weight of 4-7 mg), was pre-swelled in an HCl solution at pH 2 for 48 hours. After the swelling, the sample was soaked in distilled water for 1.5 hours, changing the water every 30 minutes, and set on a rocking table to eliminate the HCl from the chitin. The sample was then soaked in a 0.5 $mg \cdot ml^{-1}$ lectin solution in 50 mM phosphate buffer at pH 7.4. The volume of the solution used gave a final WGA/chitin ratio of 5 wt.%. The mixture was shaken on a rocking table for 72 hours at RT in a dark room. Hereafter, the sample was washed three times with 150 µL of the buffer, soaking the sample for 30 minutes each time, then dried in a desiccator and stored at 4 °C.

Samples performed:

- ‘control of chitin’: a chitin exposed to a solution with no lectin;

- 'chitin + WGA control’: a chitin sample exposed to the pristine lectin (WGA);

- ‘chitin+ WGA-RGD 1:5’: a chitin exposed to a lectin was then functionalized using a CGRGDS peptide (using a 1: 5 ratios of peptide to coupling reagents)

- ‘chitin+ WGA-RGD 1:5’: a chitin exposed to a lectin was then functionalized using a CGRGDS peptide (using a 1: 50 ratios of peptide to coupling reagents)

Collagen-based scaffold

The following steps have been realized in collaboration with the Centre the Recherche, Hôpital Maisonneuve-Rosemont, Montreal, Canada. Those corneal implants can be manufactured from a collagen-like peptide-polyethylene glycol hybrid (CLP-PEG) and inflammation-suppressing polymeric 2-methacryloyloxyethyl phosphorylcholine (MPC). Those CLP-PEG MPC implants led to reduced corneal swelling, neovascularization and haze in comparison to CLP-PEG only implants when tested into mini pigs [75] (Fig. 9). Thus, in our experiments we considered the CLP-PEG MPC hydrogel as our condition to test, and the CLP-PEG hydrogel as our control on scaffold.

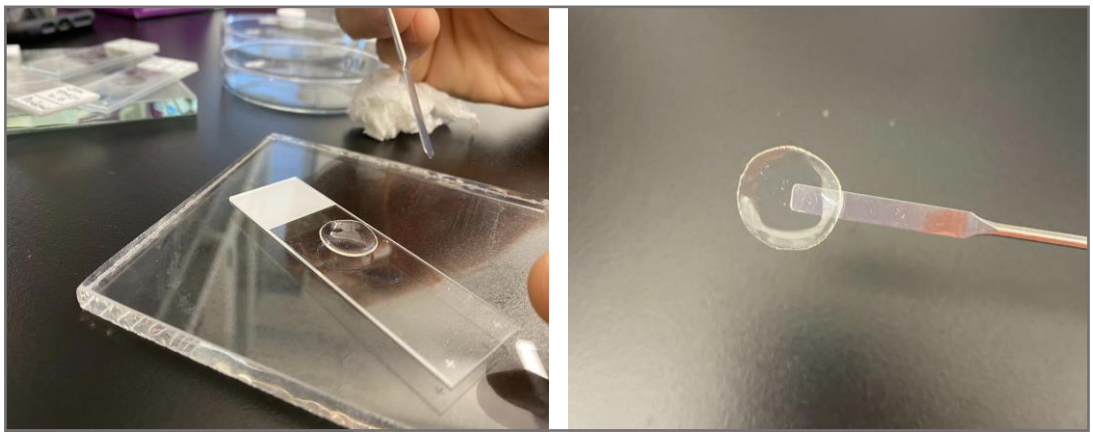

Fig. 9 Aspect of collagen-based scaffolds after preparation steps.

CLP-PEG scaffolds

CLP (CG(PKG)4(POG)4(DOG)4) (AmbioPharm, SC, USA) was conjugated to an 8-arm poly (ethylene glycol) with a hexaglycerol core (Sinopeg Biotech Co. Ltd., Beijing, China). In brief, CLP was conjugated to PEG at pH 4.5, sterile filtered and dialyzed using a 12–14 kDa membrane to remove unreacted CLP. The product was lyophilized and re-dissolved at 12% (w/w). CLP-PEG hydrogels were produced using 4-(4,6-dimethoxy-1,3,5-triazin-2-yl)-4-methyl- morpholinium chloride (DMTMM) at molar ratio of 1:2 CLP-PEG: DMTMM. Corneal implants were cast as 10 mm and were realized flat to assist a homogeneous cell seeding, 500 µm thickness.

CLP-PEG MPC scaffolds

CLP-PEG-MPC implants were manufactured using an additional phosphorylcholine network based on the interpenetrating network from our previous recombinant human collagen type III-phosphorylcholine implants. The phosphorylcholine network is composed of 2-methacryloyloxyethyl phosphorylcholine (MPC) (Paramount Fine Chemicals, Beijing, China) and polyethylene glycol diacrylate (PEGDA) (Sigma-Aldrich, St. Louis, MO). The ratio of CLP-PEG:MPC was 2:1 (w/w) and MPC:PEGDA was 3:1 (w/w). Ammonium persulfate and N,N,N'N''- tetramethylethylenediamine (Sigma-Aldrich, St. Louis, MO) were both used as polymerization initiators at a ratio of MPC:APS of 1:0.03 and APS:TEMED of 1:0.77. Corneal implants were cast as 10 mm and were realized flat to assist a homogeneous cell seeding, 500 µm thickness.

Cultivation of Human Corneal Epithelial Cell Line (HCEC)

The supplemented Keratinocyte SFM (KSFM) was prepared adding entire contents of the BPE and EGF supplement vials to a 500mL bottle of Keratinocyte SFM basal medium, with the addition of 5.0 mL 100X Antibiotic-Antimycotic to the supplemented medium. The cells were seeded at 5.000/cm^2. The medium was changed every two days until 80%-90% of confluence is reached. HCEC typically take 5–7 days to reach confluence under these conditions. To detach cells TrypLE^{TM} dissociation reagent was used and cells were incubated at 37°C for 6-8 minutes. Then, cells were centrifuged at 180 × *g* for 5 minutes at RT (Fig. 10).

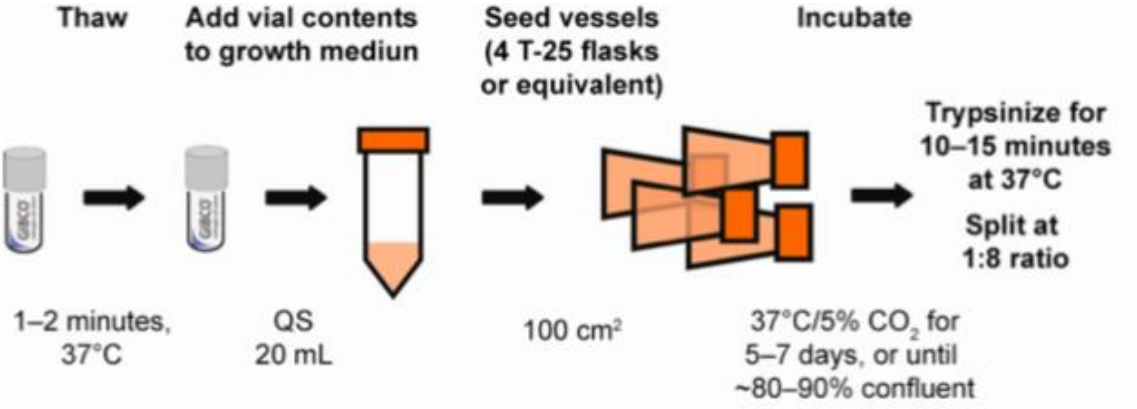

Fig. 10 Thermofisher Scientific protocol for HCEC cell line

The use of 3T3-J2 cell line for human primary cultures

Limbal epithelial cells were cultivated on a lethally irradiated feeder layer 3T3-J2 cells (a gift from Prof. Howard Green). The culture system, first described by Rheinwald and Green in 1975 [35], is composed by lethally irradiated 3T3 cells at the correct density, that together with the right cell culture medium, helps the expansion of keratinocytes from a small biopsy.

During serial cultivation, the 3T3-J2 murine fibroblast cell line was defrosted, amplified and maintained in Dulbecco Modified Eagle Medium (DMEM; EuroClone) supplemented with 10% irradiated Donor Bovine Serum (DBS; Thermo Fisher Scientific), 4mM glutamine (EuroClone) and 50IU/mL penicillin/streptomycin (EuroClone). Before being used as F/L, cells were subjected to lethal radiation at ~60Gy and then plated at standard concentrations.

Human limbal biopsy collection and primary cultures of human limbal stem cells

Human limbal epithelial cells were obtained from human donor biopsies, after informed consent. Each biopsy was collected from the physician, cleaned and preserved in storage medium (Eusol-C, CSM 001-00, Alchimia s.r.l.) that is a fully synthetic medium for corneal storage at 4 °C suitable for up to 14 days. Biopsies were collected from the physician within 24 hours following the death of the patient and delivered to the laboratory at 4°C. Upon arrival, the biopsies were kept in the fridge at 4°C for maximum 14 days. Each biopsy was subject to mycoplasma test at the arrival in the laboratory. The test was performed through MycoAlert® Mycoplasma Detection Kit (Lonza) on the GloMax®-Multi+ Detection System with Instinct™ Software.

Each biopsy was usually treated under sterile condition. The limbus zone was separated from the corneal zone and the conjunctiva and washed in sterile Dulbecco-phosphatase buffer saline (D-PBS 1x, Gibco, Thermofisher, 500ml) 2-3 times. Then, the biopsy was dissociated in 0.05% trypsin (Thermo

Fisher Scientific, Waltham, Massachusetts, USA) and 0.01% 2,2′,2″,2‴-(Ethane-1,2-diyldinitrilo) tetra-acetic acid (EDTA) at 37°C for 4 cycles. After each cycle, cells were collected every 30 minutes and centrifuged at 2900 rpm for 5 minutes at RT. The pellet was re-suspended in the dedicated medium.

Cells were plated (1.5 x 10^4/cm^2) on lethally irradiated 3T3-J2 cells (2.4 x 10^4/cm^2) and cultured in 5% CO^2 and in 95% humidified atmosphere. The medium used for biopsy collection and cell cultivation is the so-called keratinocyte growth medium (KNO) composed by DMEM and Ham's F12 (EuroClone, Milan, Italy) media with a 2:1 ratio. Additionally, this medium contains fetal bovine serum (10%) (FBS; Thermo Fisher Scientific), insulin (5 mg/mL) (Eli Lilly and Company, Indianapolis, Indiana, USA), adenine (0.18 mM), hydrocortisone (0.4 mg/mL), cholera toxin (TC) (0.1 nM), triiodothyronine (T3) (2 nM), glutamine (4 mM) (EuroClone, Milan, Italy), and penicillin/streptomycin (50 IU/mL) (EuroClone, Milan, Italy).

Epidermal growth factor (EGF) (10 ng/mL) was added at 10 ng/mL to the KNO medium at the first feeding, 3 days after plating (the so-called KC medium after adding the EGF). Cultures were then fed every couple days with the selected KC medium. In serial propagation assays, sub-confluent primary cultures were passaged when subconfluence is reached at a density of 6 x 10^6 cells/cm^2 and cultured as above. Cells were dissociated at 37°C with TE 10x dilute 1:10 in D-PBS for 15 minutes and serially cultivated until replicative senescence was reached [27]. In case of cells were frozen at -196°C, they were suspended in freezing medium composed by KNO medium with the addition of 10% glycerol (Johnson & Johnson, New Brunswick, New Jersey, USA). All the reagents used for the cell extraction and culture were extensively selected and screened for the contaminants and cytotoxic effects absence.

Colony-forming Efficiency (CFE) Assay

A small quantity of cells (100-2.000) from the single biopsy and from every cell passage of serially propagated mass were plated in a couple of 100mm^2 cell culture dishes onto 3T3 F/L cells and cultivated as explained above. The grown colonies were fixed after 12 days of cultivation, stained with rhodamine B (Sigma-Aldrich, St. Louis, Missouri, USA) and scored under dissecting microscope. Values of colony forming efficiency were calculated as the ratio of the grown colonies on the number of inoculated cells. All colonies were scored whether progressively growing or aborted [26, 27].

Acute and Chronic toxicity evaluation on scaffolds

Both the acute and chronic toxicity evaluation were performed sub-cultivating the cell cultures for several passages on plastic after one or more passages on the scaffold material in comparison to the control condition on plastic (as shown in figure 11).

The keratinocytes cell type was seeded onto the scaffold coated as previously described and previously seeded with F/L cells. The KC medium was changed first at day three and then every two days until sub-confluence was reached. After enzymatically detaching the cells through trypsinisation

at 37° for 15 minutes, an aliquot of cells was placed in indicator dishes for the CFE assessment. On the other hand, the remaining cells were serially sub-cultivated for further three passages with standard culture conditions on plastic to evaluate a possible cell recovery in case of acute toxicity.

Instead, to perform the chronic toxicity assay, the keratinocyte cells were seeded onto the scaffold coated as previously described and previously seeded with F/L cells. Then, keratinocytes were enzymatically detached by trypsinization at 37° for 15 minutes. An aliquot of cells was placed in indicator dishes for the CFE assessment. The remaining cells were serially sub-cultivated for further three passages; half onto another same scaffold material and half on plastic material, at every detachment. Both conditions were cultivated with our standard culture conditions (seeding F/L cell type previously and after the keratinocyte cell type) for cell recovery evaluation.

Moreover, during all cell recovery passages, an aliquot of cells was collected and pelleted for western blot analysis, a small aliquot was collected for cytospin analysis of p63 and another one was plated onto glass slide coverslips for subsequent immunohistochemical analysis.

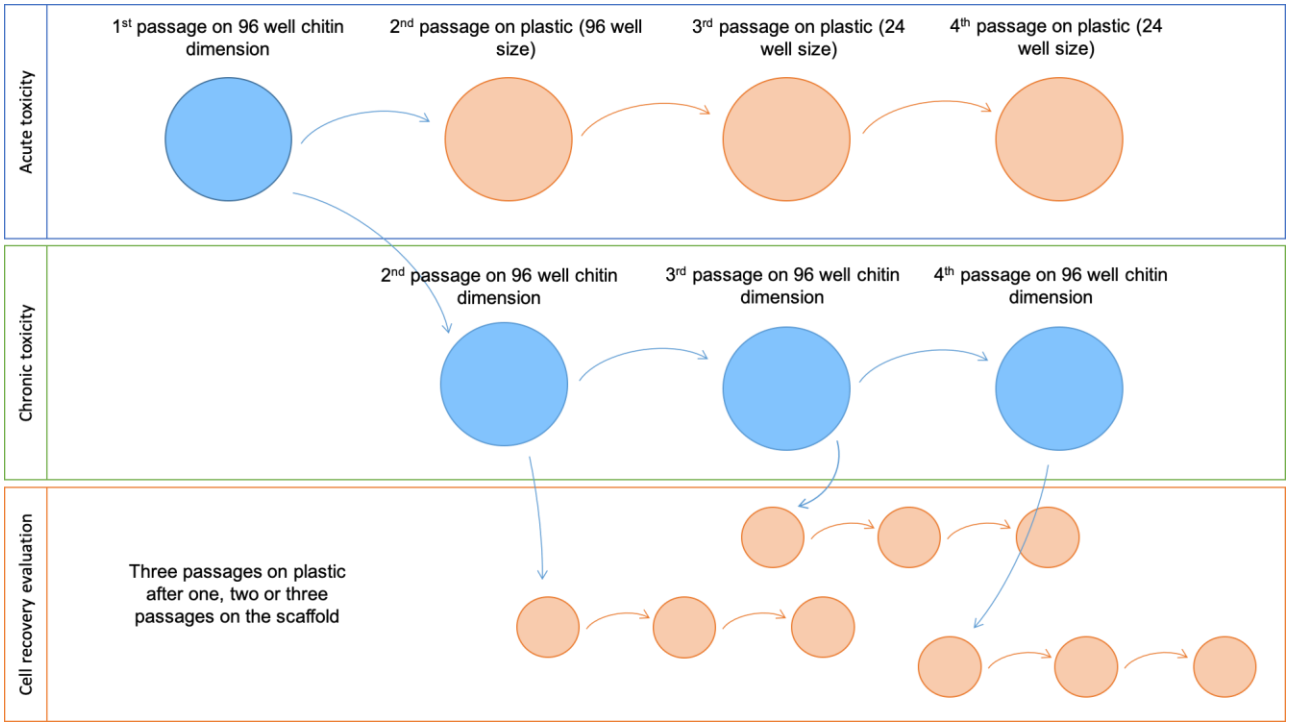

Fig. 11 Acute and chronic toxicity representation.

Immunohistochemistry analysis

Human keratinocytes samples grown on plastic and on the selected scaffolds, were equilibrated in sucrose 15% for 1 hour, sucrose 20% for 1 hour and then sucrose 30% O/N, then included in OCT compound (optimal cutting temperature compound, killik; Bio-Optica, Milan, Italy). The embedded samples were cut to obtain 8-10 µm-thick sections with a cryostat (Leica 1850 UV). These sections and glass slide coverslip were fixed with 3% paraformaldehyde for 10 minutes at RT or cold methanol for 10 minutes at -20°C. Glass slides and coverslips were then permeabilised with 0.5-1% Triton X100

in PBS 1x (10 minutes at RT), incubated with primary antibody for 30min at 37°C; dilution of antibodies are show in Table 4. The appropriate secondary antibody was then added for other 30min at 37°C (Alexa-Fluor 488 and Alexa-Flour 568). The nuclei were labelled with 4',6 diamidino-2-phenylindole (DAPI) for 5 min and the samples were mounted with Dako mounting medium (Sigma-Aldrich) on microscope slides.

The images of epithelial cultures were acquired with a laser-scanning confocal microscope (LSM 900, Zeiss).

Primary Antibody	Source	Dilutions	Species
CK3	Abcam	1:100	Rabbit
CK14	Biolegend	1:1000	Rabbit
P63α	Primm (customized)	1:5000	Rabbit
Laminin 5	Abcam	1:400	Rabbit
14-3-3-Sigma	Abcam	1:200	Mouse

Table 4 Primary antibodies used

The p63-bright cells analysis

This method is a rapid and sensitive Q-FIHC assay for the detection and quantification of fluorescent intensity in human corneal tissues and cells obtained from small human samples. Since p63α has been recognized as a limbal stem cell marker, the accurate and fast determination of its abundance is crucial to evaluate the quality (defined by the stem cell content) of the epithelial culture [Di Iorio, 2006 #72].

Primary cultured human limbal keratinocytes cells were trypsinised, collected and 10.000 cells/glass slide were placed via Cytospin (Thermo scientific) onto a Shandon glass slide, and fixed in PFA for 10 minutes at RT. Slides were let dry in air and then washed with PBS 1x for 10 minutes each of the three washes. Samples were stored at +4°C in PBS 1x + Azide (Thermofisher Scientific) for future analysis [76].

Immunofluorescence of p63

The cytocentrifugates were incubated with primary antibody against human p63α for 1 hour at 37°C. Fluorescence-conjugated secondary antibody (Alexa – Fluor 488) was incubated for 1 hour at RT. Coverslips were placed on the slides. Fluorescence labelled signals were acquired using the Zeiss

imager A1 fluorescence microscope. Acquisition requires all the cells to be in a single focal plane. The cells should be individually resolvable, not in clusters or clumps. Image analysis was performed using AxioVision software v.4.5 (Jena,Germany).

Western Blot Analysis

Proteins from all cultures were extracted from dry pellets by RIPA buffer (Sigma), phosphatase and protease inhibitor (ThermoScientific) at 0–4°C.

Equal protein amounts were electrophoresed on NuPage 4-12% Bis-Tris Protein gels (Life Technologies) and transferred to nitrocellulose membranes (Life Technologies). Protein bands immunoreactions were performed with different primary antibodies (Table 5) and the corresponding HRP-conjugated secondary antibody (donkey anti-rabbit, Santa Cruz Biotechnologies, sc-2313, goat anti-rabbit, Abcam, ab2057, donkey anti-mouse, Abcam, ab6789). Proteins signals were developed using a chemiluminescent labelling reagent (Super Signal West Pico Chemiluminescent Substrate, Thermo Scientific) and acquired with ChemiDoc™ MP Imaging System (BIO-RAD), while bands quantification was performed with Image J software.

Primary Antibody	Source	Dilution	Species
P63-alpha	Primm (customized)	1:5000	Rabbit
BMI-1	Cell Signaling	1:500	Rabbit
CK14	Biolegend	1:40000	Rabbit
Involucrin	Leica	1:1000	Mouse
GAPDH	Abcam	1:10000	Mouse
Vimentin	Biolegend	1:1000	Rat

Table 5 Primary antibodies used in western blot analysis

Results

Between others, Builles et al. presented some experiments with scaffolds consisting of orthogonally aligned multilayers of collagen fibrils prepared in a high magnetic field. The group performed those experiments to perfectly mimic the corneal matrix to properly reconstruct an *in vitro* human Hemi-cornea (stroma and epithelium). However, these tests showed that although the scaffold matrix was mocked similarly to the native cornea, the result in biomechanical and cell integration terms was relatively poor [77]. Therefore, we focused on the material's properties regardless of its three-dimensional chemical structure.

An analysis of the different biomaterials led us to select a biomaterial of marine origin for its extraordinary transparency and for its lamellar structure, which reproduce the corneal structure and which have essential biomechanical characteristics and resistance even higher than those of the native cornea. The squid pen (gladius) from the *Loligo Vulgaris* was used for the preparation of β-chitin materials [4].

Also, to make suitable the material for our cell type, modifications of the material were carried out on the surface. In fact, surface variation of materials with bioactive molecules allows to have biomimetic materials. The bioactive molecules could be whole ECM molecules or "cell-binding" domain sequences isolated from these proteins. The experiments performed relate the study of the cell attachment, proliferation, spreading, and differentiation on selected modified materials, providing a suitable environment for epithelial cells as it mimics the 3D environment of the natural ECM.

Chitin scaffold: functionalization with Collagen IV and human fibronectin

Based on previous experiments performed in our laboratory, we decided to functionalize the chitin material with two essential proteins useful for cell binding: collagen IV and fibronectin.

After the deproteinization and sterilization step, the chitin material was functionalized with a mix of collagen IV and human fibronectin, as explained in this manuscript's materials and methods section and as presented figuratively in fig. 12 A. To evaluate the functionalization's effect on cell growth and adhesion, we cultivated human limbal keratinocytes onto the selected scaffold for one passage (passage III). Then, we serially cultivated the keratinocytes cells (collected from the biomaterial) on plastic from passage IV to VIII (referred to as "recovery" passages) (fig. 12) to observe if the chitin material caused acute toxicity. We compared this condition with serially cultivated passages on plastic control conditions (from passage III to passage VIII) and prepared CFE at each passage for both conditions. We analyzed clonogenic and aborted colonies generated by cells grown on the plastic condition and the scaffold. In particular, CFE results showed a decrease in cells grown on the scaffold, an increase of the aborted colony number, and a reduction of clonogenic cells compared to the plastic culture plate (fig. 12 D). These data highlighted that the cell adhesion was not stable and not comparable to the control condition on plastic and performing the same number of passages an early

clonal conversion, due to lack of cell adhesion, occurred (fig. 12E). In conclusion, our primary goal after those experiments was to implement and stabilize the epithelial cell adhesion on the scaffold.

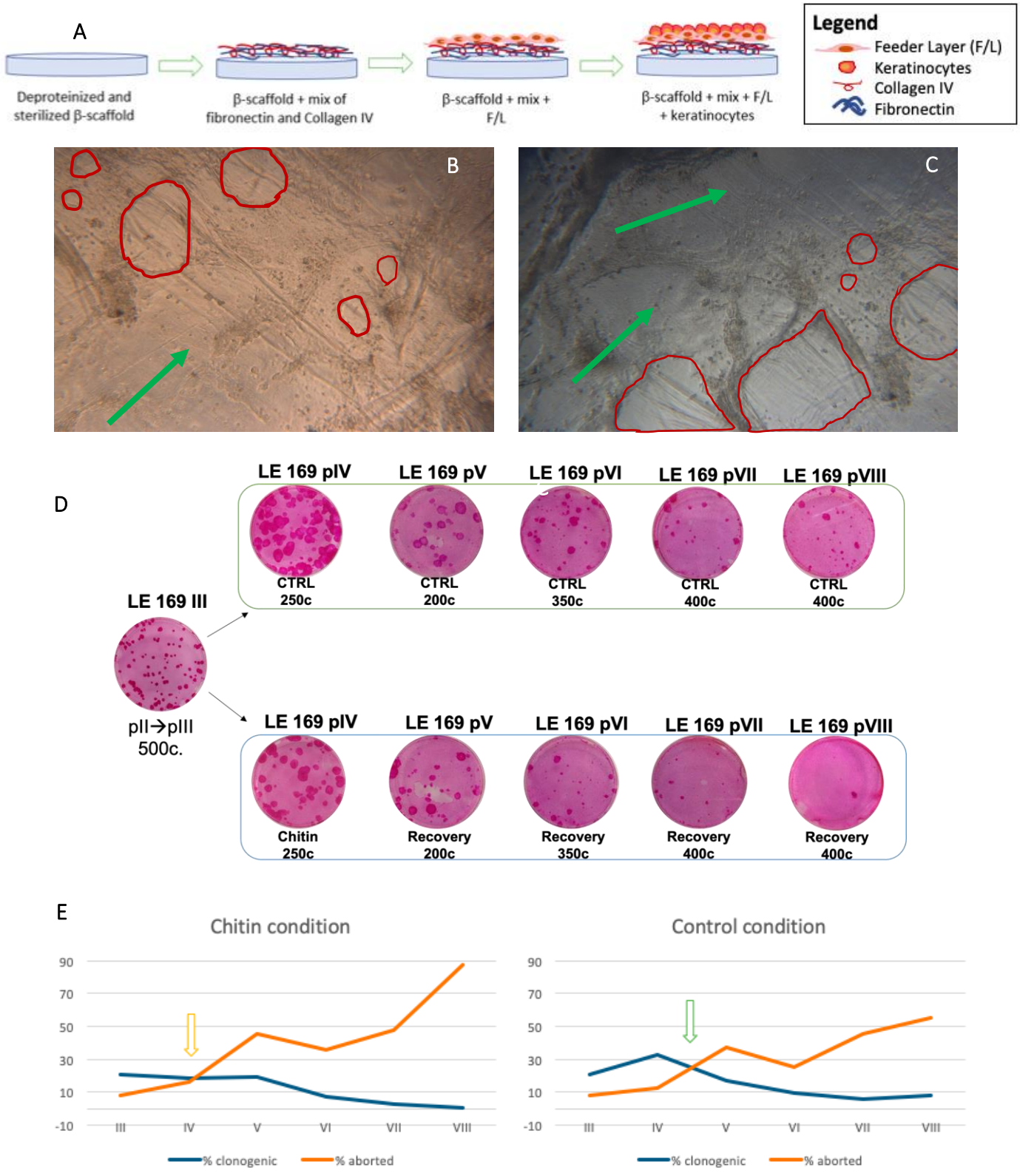

Fig.12 A: scheme of the functionalization protocol. B-C: At day 5, on top of the chitin scaffold functionalized with collagen IV and human fibronectin the adhesion was not homogeneous (marked in red). There were cell colonies (green arrows).

D: representative pictures of CFE assay for both conditions. E: Comparing colony-forming efficiency assay of the control condition and the selected scaffold condition after several passages. There is clear a decrease in cells grown on the selected scaffold; thus, an increase of aborted colony number and decrease of clonogenic cells compared to the control culture on plastic.

Thus, we decided to move towards another type of functionalization. Specifically, we tried the aptamers, linking systems already known to promote stable adhesion between the cell and the matrix.

Critical improvements in the aptamer technology have played an essential role in identifying development candidates with suitable properties: aptamers can bind non-covalently with high affinity and specificity to a target molecule [78].

Specifically, aptamers are single-stranded oligonucleotides that can selectively recognize targets ranging from small compounds proteins to whole cells. They represent three significant advantages: (i) access to membrane proteins in their native conformation similar to the *in vivo* conditions, (ii) natural selection without prior purification of membrane-bound targets, (iii) identification of (new) targets related to a specific phenotype [79] and even if the study of biomaterials coated with aptamers is a less explored field in the literature, it has great promising potential.

Chitin scaffold functionalization with aptamers

Thus, we decided to test two types of aptamers, one screened against fibronectin (referred to aptamer anti-laminin) and the other screened against laminin 5 (referred to aptamer anti-fibronectin). These experiments aimed at investigating whether immobilized anti-fibronectin aptamers or immobilized anti-laminin aptamers could promote the adhesion and growth of keratinocytes cells onto the selected chitin scaffold. Significantly, although the use of anti- fibronectin aptamers has been previously shown to serve as a tool to inhibit cell adhesion by impeding the interaction of integrins with cell binding domains [80], this is one of the first reports of aptamers directed against fibronectin to improve cell adhesion on a scaffold [81].

Briefly, we tested different protocols:

- the chitin functionalized with aptamer anti-laminin where were added respectively:

- exogenous laminin 332 or 511 (fig. 13 A)
- endogenous laminin produced by the keratinocyte cell type (fig. 13 B)

Referred to as conditions C1 and C2 of materials and methods section.

- the chitin functionalized with aptamer anti-fibronectin, where was added:

- exogenous human fibronectin (fig. 13 C)

Referred to as condition B1-2 of materials and methods section.

The presence of aptamers on hydrogels was confirmed using an UV-fluorescence DNA intercalating dye (SYBR Safe DNA gel stain, Life Technologies, Carlsbad, CA; USA) (fig. 14).

PRO	CONS
They can bind to the target with high affinity and specificity[1]	
Chemical modifications can be done to reduce their susceptibility to degradation by nucleases in serum[3]	In vivo: Vulnerable to degradation (as they are nucleic acids) especially for RNA-based aptamers [1]
The biodistribution and the clearance of aptamers can be altered by the chemical addition of polyethylene glycol and other moieties[3]	Used more the DNA-based aptamers. The DNA molecules are naturally resistant to 2'-endonucleases[1]
Enhanced permeability and retention effect[1]	The conformational diversity of nucleic acids is limited more than that of monoclonal antibodies[2]
Faster tissue penetration, virtual non-immunogenicity, ease of conjugation or modification [1,2]	Nucleic acid aptamers with highly negative charges have difficulty binding with the negatively charged target molecules[2]
Simple and low-cost chemical synthesis [1]	
Wide range of potential biological targets[1]	
They have a small size and nucleic acid characteristics that can improve their clinical applicability and suitability for industrialization[2]	
They **are nontoxic in vivo**[2]	
Thermal stability (they can be heated up to 80°C or stored in various solvents and they will return to their original conformation) [3]	

(1) Aptamers and their applications in nanomedicine, Hongguang et al. *Small 2015, 11, No.20, 2352-2364*; (2) A highlight of recent advances in aptamer technology and its application, Hongguang et al. *Molecules 2015, 20, 11959-11980*; (3) Discovery and development of anticancer aptamers, Ireson et al. *Mol Cancer Ther 2006; 5(12).*

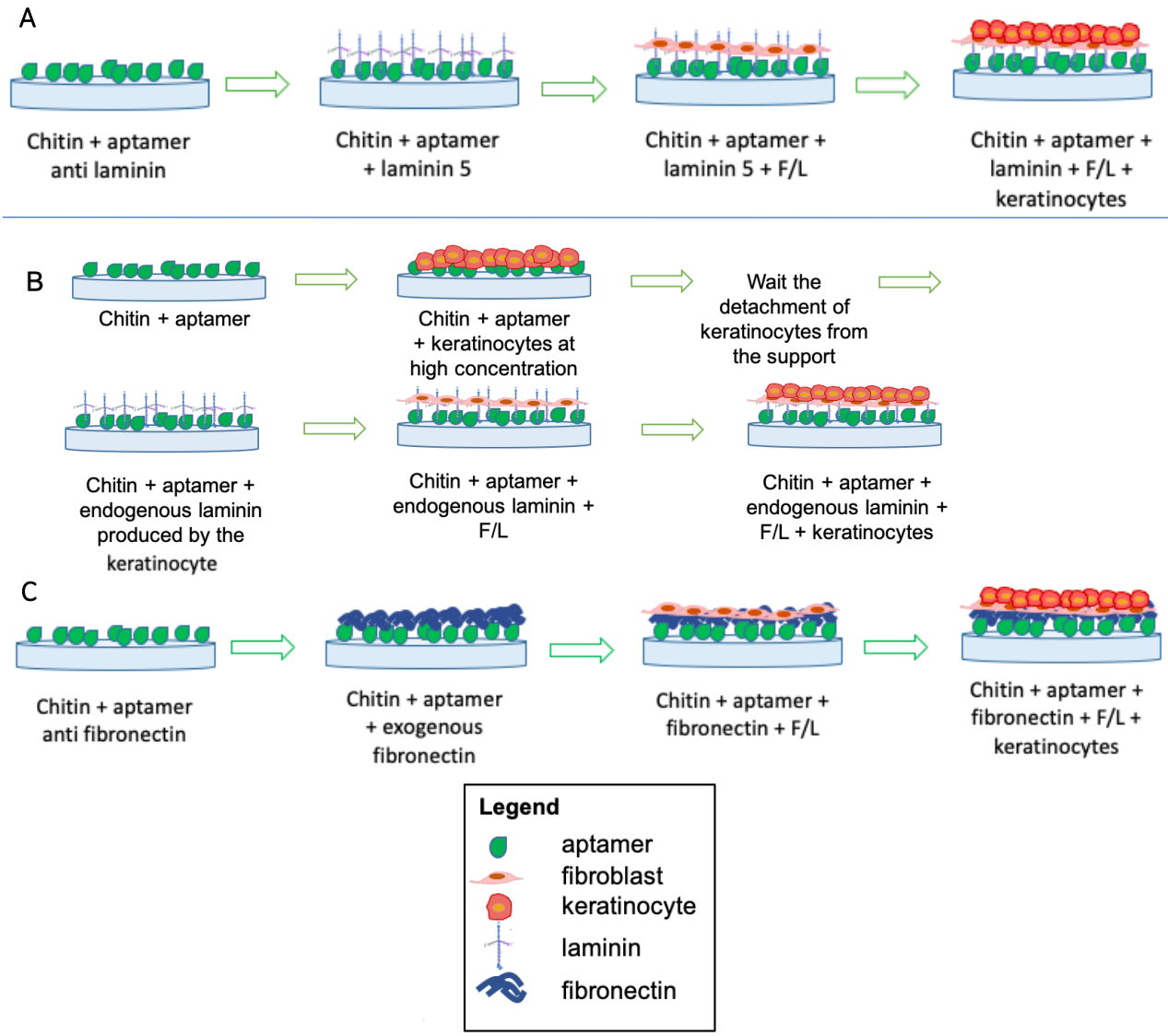

Fig. 13 Design of the experiment (A) exogenous laminin 5 (BioLamina) and aptamer-anti laminin as a scaffold functionalization; (B) endogenous laminin and aptamer anti-laminin as a functionalization step and (C) exogenous human fibronectin linked to aptamer anti-fibronectin as a scaffold functionalization.

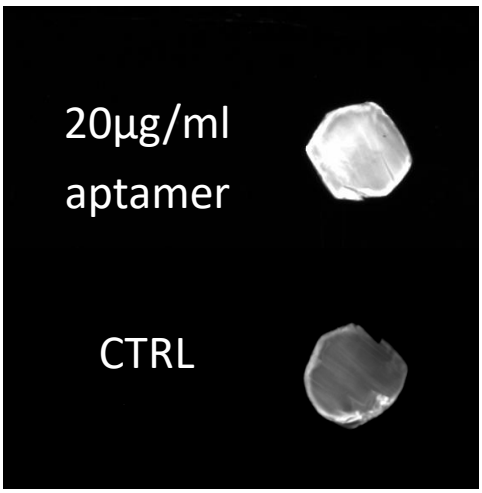

Fig. 14 The presence of aptamers on hydrogels was confirmed with an UV-fluorescence DNA intercalating dye

Chitin scaffold: functionalization with aptamer anti-laminin

In this series of experiments, customized ssDNA aptamers were screened against human laminin (ATW0024, Base Pair Biotechnologies, Pearland, TX) and modified with a short carbon chain containing a disulfide bond on their 3′ end and with biotin on their 5′. Aptamer sequence is a property of Base Pair Biotechnologies and could not be disclosed in the present manuscript.

After the deproteinization step with NaOH 1M and the sterilization step in an autoclave, the chitin scaffold was functionalized with the aptamer anti-laminin, as explained in the materials and methods section. Then, the functionalized material was coated with exogenous laminin 332 or 511 (BioLamina).

To investigate whether scaffolds functionalized with aptamers could be enriched for the target protein laminin, they were coated with 20 µg/ml of aptamer and incubated with respectively 5 µg/ml - 10 µg/ml - 15 µg/ml concentrations of laminin 332/511, based on the protocol of the BioLamina company where the suggested concentration of laminin for coating was between 5 to 10 µg/ml. Also, the endogenous laminin produced by the keratinocyte was considered as a coating in a similar condition after adding the aptamer screened against laminin (Fig. 13 B). The keratinocyte usually produces endogenous laminin, so we seeded a high percentage of keratinocytes to obtain a «natural» laminin-coating (fig. 15).

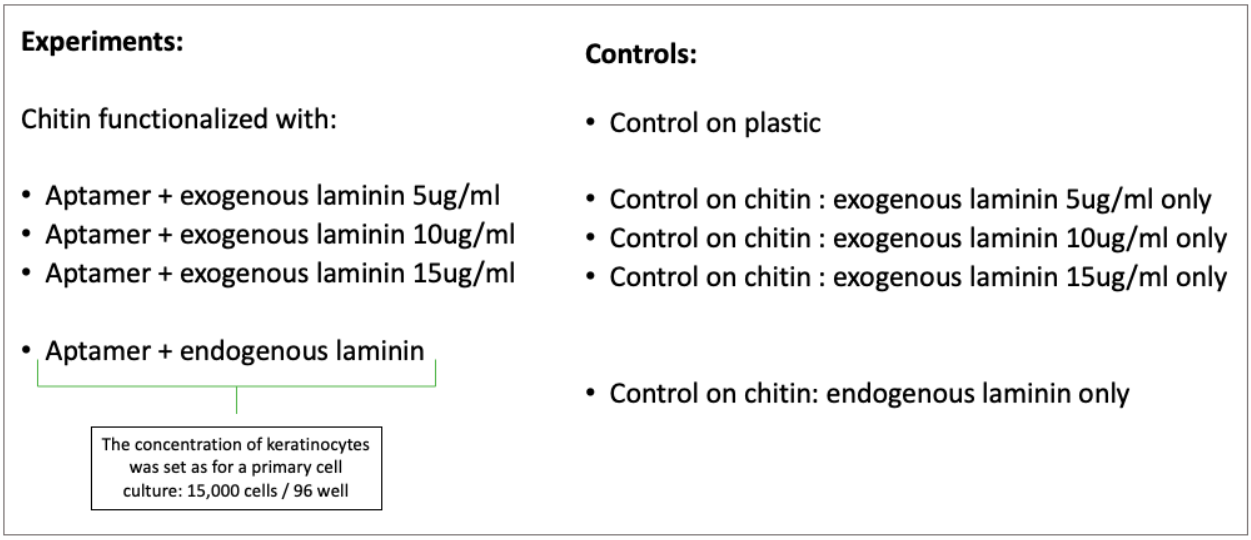

Fig. 15 Design of the experiment

The condition with 5 µg/ml of laminin 332 was considered the best one compared to the others. As presented in figure 16 A, some Feeder Layer cells adhered to the scaffold. However, that condition was still not optimal for keratinocytes cell growth. Instead, conditions with a higher concentration of laminin, and the condition with endogenous laminin production, were not adequate for both F/L and keratinocytes cell growth (fig. 16 B and C). To confirm the correct functionalization with laminin 5, an immunofluorescence analysis was performed to confirm the continuous disposition of laminin 5 onto the scaffold (fig. 17).

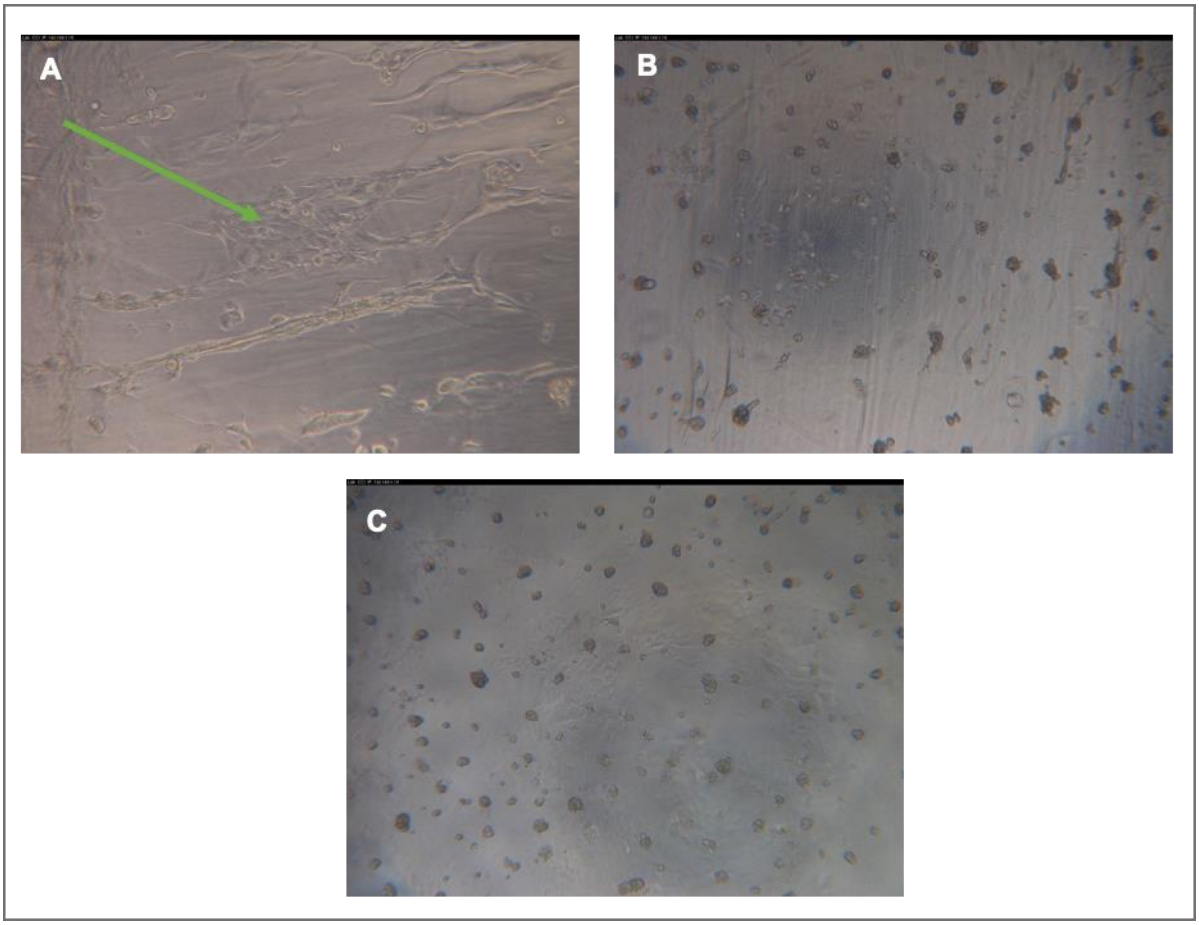

Fig. 16 (A) aptamer and exogenous laminin 5 µg/ml; (B) representative picture for the same result observed for both aptamer and exogenous laminin 10 µg/ml and 15 µg/ml; (C) aptamer and endogenous laminin

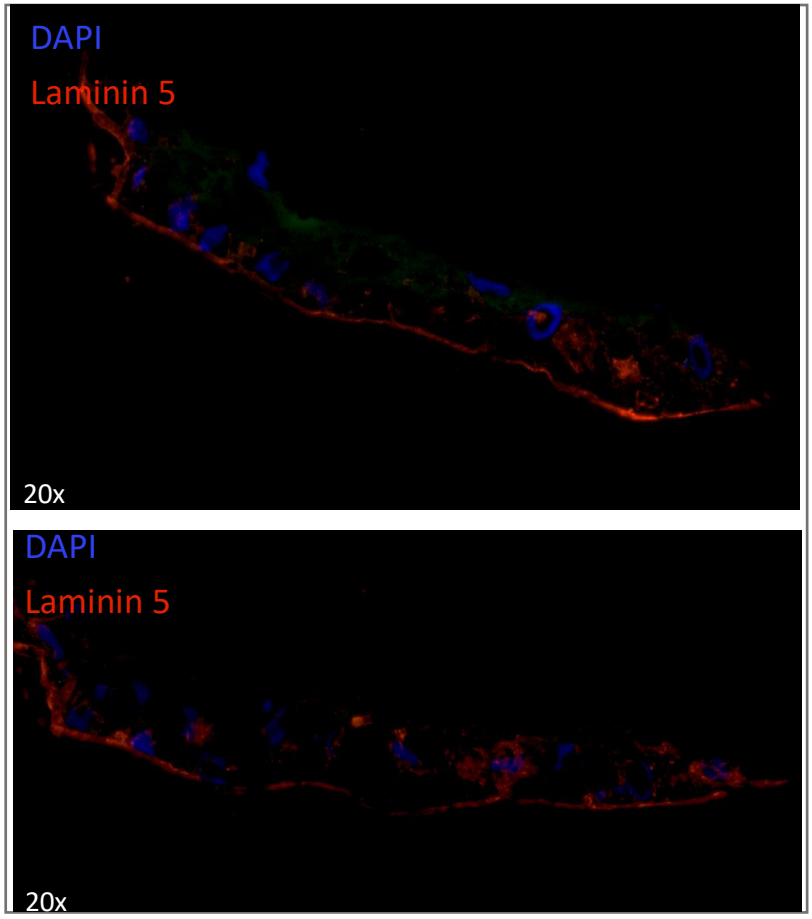

Fig. 17 5 µg/ml exogenous laminin with aptamer and F/L seeding at day two of culture.

Thus, we decided to implement the 5 µg/ml laminin condition, trying to analyze if the F/L cell type was in some way a hindrance for exogenous laminin-based attachment of keratinocytes (fig. 18). We decided to test two conditions: one comparable to the standard culture condition where F/L seeding was followed by keratinocytes seeding (fig. 18 A) and one with only keratinocytes seeding (fig. 18 B). Both combinations produced the death of cells, and no cell colonies were observed compared to the control condition.

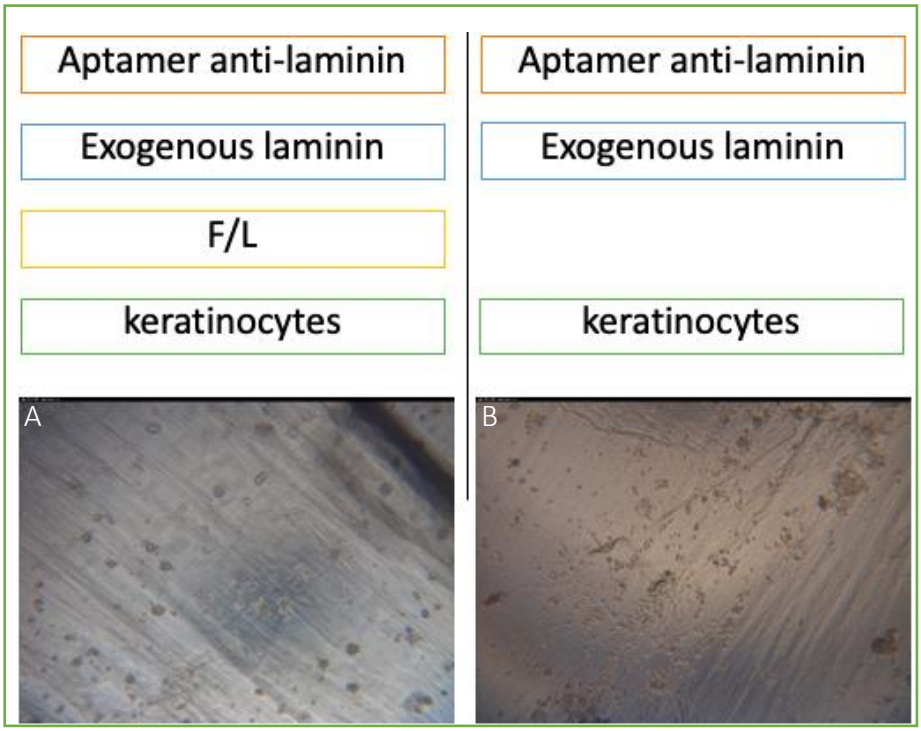

Fig. 18 (A) condition with F/L and keratinocytes; (B) condition with keratinocytes only. Pictures are at day five of culture.

In conclusion, despite these innovative aptamer tools, in this condition we could not stabilize the adhesion of the corneal epithelial cells, due to their specific requirements. In fact, *in vivo,* the matrix of the limbus where stem cells reside is different from the cornea matrix where there are no stem cells. Thus, even in this case, the cell adhesion on the selected scaffold must be refined since it was not sufficiently stabilized.

For this reason, we decided to test the aptamer screened against human fibronectin since few examples of its use were already described in scientific literature [81].

Chitin scaffold: functionalization with aptamer anti-fibronectin

In this block of experiments, we used ssDNA aptamers screened against Fibronectin (ATW008 Fibronectin aptamer, Base Pair Biotechnologies, Pear- land, TX) and modified with a short carbon chain containing an S-S bond on their 3' end and with biotin on their 5'. Aptamer sequence is a property of Base Pair Biotechnologies and could not be disclosed in the present manuscript.

We functionalized the chitin scaffold with different quantities of aptamer anti-fibronectin: 10 µg/ml, 20 µg/ml, 40 µg/ml to understand which concentration was the best for keratinocytes growth and adhesion. Briefly, the chitin scaffold was deproteinized with NaOH 1M and then sterilized in an autoclave as previously described. Then, the aptamer anti-fibronectin was added onto the scaffold, and F/L cells and keratinocytes were seeded, as explained beforehand. In this condition, cells didn't attach properly to the material, concluding that the aptamer alone was not sufficient for F/L and keratinocytes adhesion (Fig. 19).

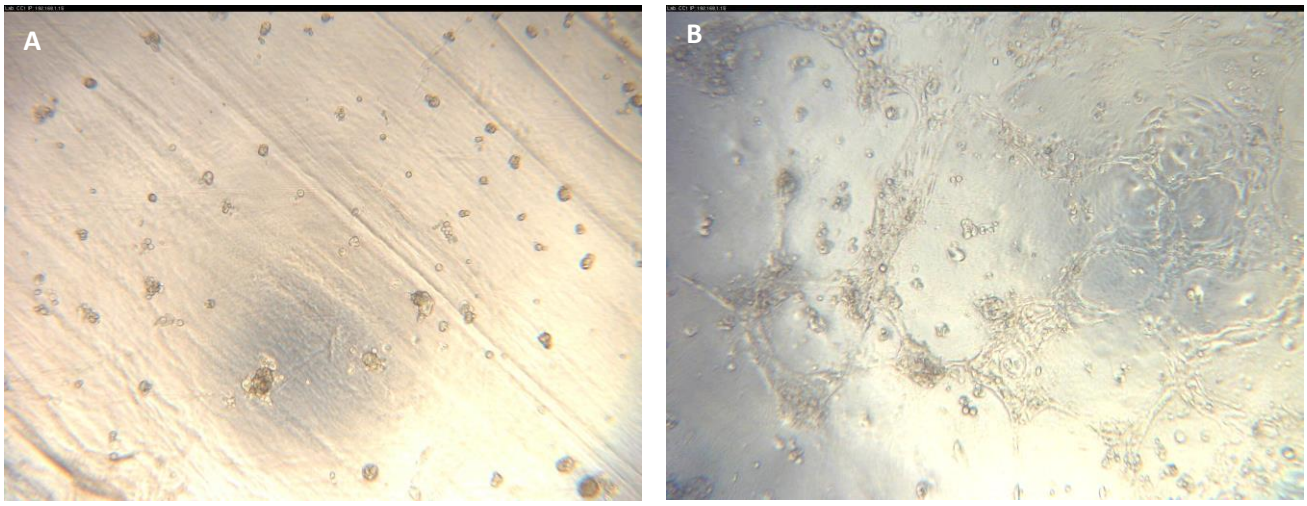

Fig. 19 Aptamers alone are not sufficient for keratinocytes adhesion. (A) representative picture of the three concentration of the aptamer on chitin scaffold tested where no cells growth was visible at day 5; (B) control on plastic at day 5, where cell colonies grown.

Then, we performed another experiment incubating 20 µg/ml of the aptamer anti-fibronectin with a 60 µg/ml of exogenous fibronectin. Different conditions were compared:

1) control on plastic

2) aptamer anti-fibronectin + exogenous fibronectin: not dried

3) aptamer anti-fibronectin + exogenous fibronectin: dried for 1 hour

The difference between conditions 2) and 3) is regarding the protocol. In condition 3) the chitin was let dry for 1 hour after adding the exogenous fibronectin, compared to condition 2).

F/L and keratinocytes were added as previously described and maintained in culture for five days on all conditions.

On day five of culture, condition 3) seemed to be comparable to the control on plastic, as presented in figure 20.

In all conditions, cells were cultivated for the first passage on chitin. Then, in condition 3), which was the only one suitable for cell growth, serial passages were performed on plastic to analyze if acute toxicity occurred. This condition was performed alongside several passages of the control condition on plastic.

From each passage of every condition, an aliquot of cells was collected for CFE analysis, western blot analysis, and quantification of p63.

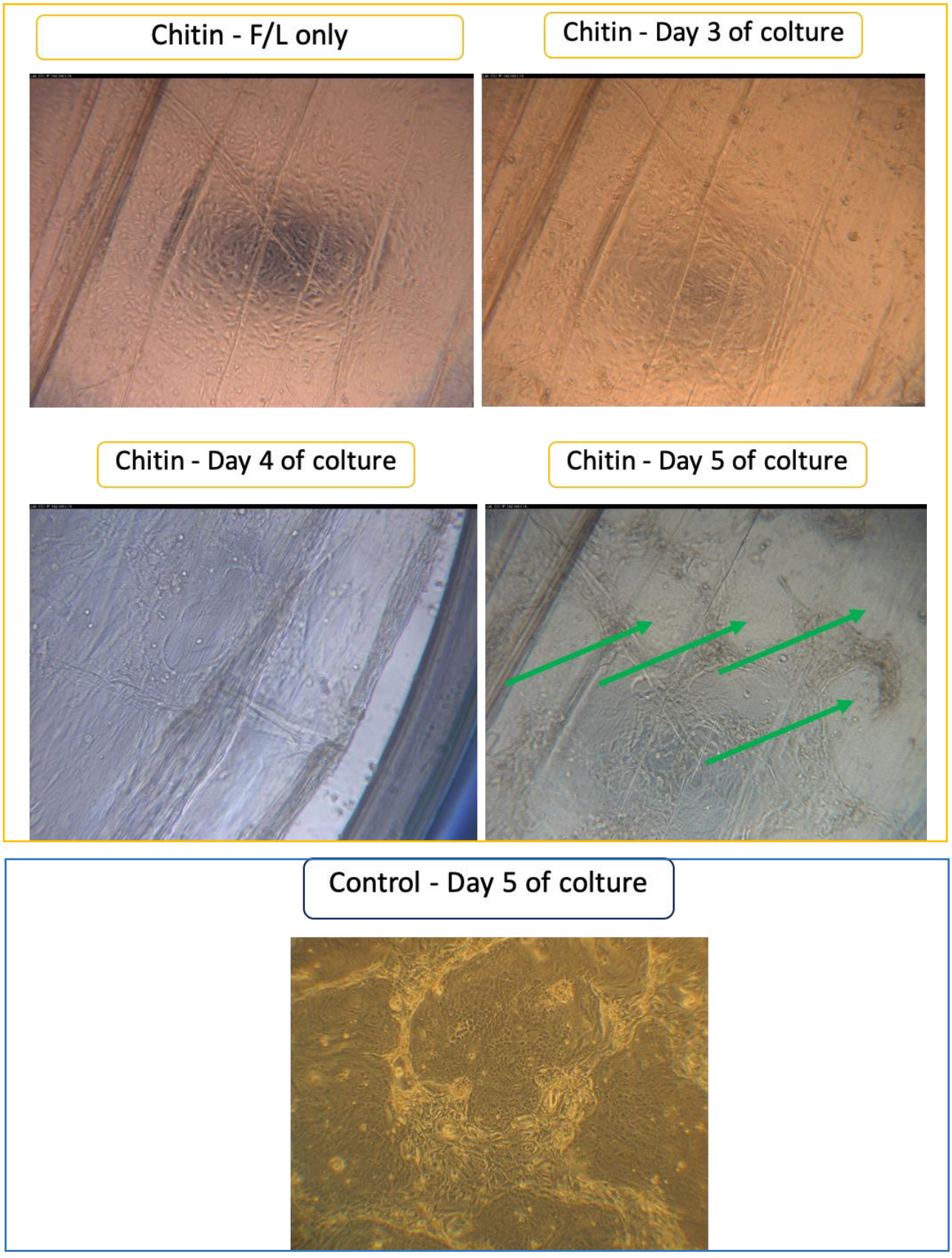

Fig. 20 Condition 3) at day five of culture, in comparison with the control condition on plastic. The condition on chitin showed comparable results to its control on plastic; there were comparable cell colonies grown onto the chitin surface (green arrows).

Cell culture quality after one passage on the scaffold

We observed that cells grown on plastic underwent the same number of serial passages (fig 21 A) and had the same behavior as those grown on the scaffold. These data highlighted that the scaffold didn't produce any toxic effect on the cells. Moreover, these results showed that cells grown on the scaffold had comparable results in western blot analysis (fig21 C) and in p63 quantification (fig 21 B) in comparison to cells grown in the control condition on plastic. Especially, in WB analysis, the protein bands of basal epithelial cell marker (CK14), early epithelial differentiation marker (involucrin), stem/progenitor cells markers (p63α; BMI-1), and F/L contamination (vimentin) were comparable with the control condition.

The markers analyzed for the cell characterization have been used to assess the identity, the differentiation status, and the quality in terms of the general content of stem-progenitor cells within the cultures derived from the serial passages onto the scaffold.

Primarily through western blot analysis, p63α expression appeared to be similar between the control condition and the chitin condition along passages and Bmi1 expression. Also, although serial passages on chitin scaffold, the basal cell marker CK14 appeared to be expressed. Similar results arise from the analysis of the epithelial differentiation marker involucrin. The involucrin expression reveals the cells' ability to undergo asymmetric division, giving rise to the differentiated cells.

In conclusion, the experiments with aptamer anti-fibronectin and exogenous fibronectin revealed an increased cells attachment than the previous tests (both the condition with the mix of collagen IV and fibronectin and the one with aptamer anti-laminin), and no significant differences have been observed between the cultures' control and the chitin conditions. However, several other studies were needed, and more standardization of the protocol and starting materials were required.

A

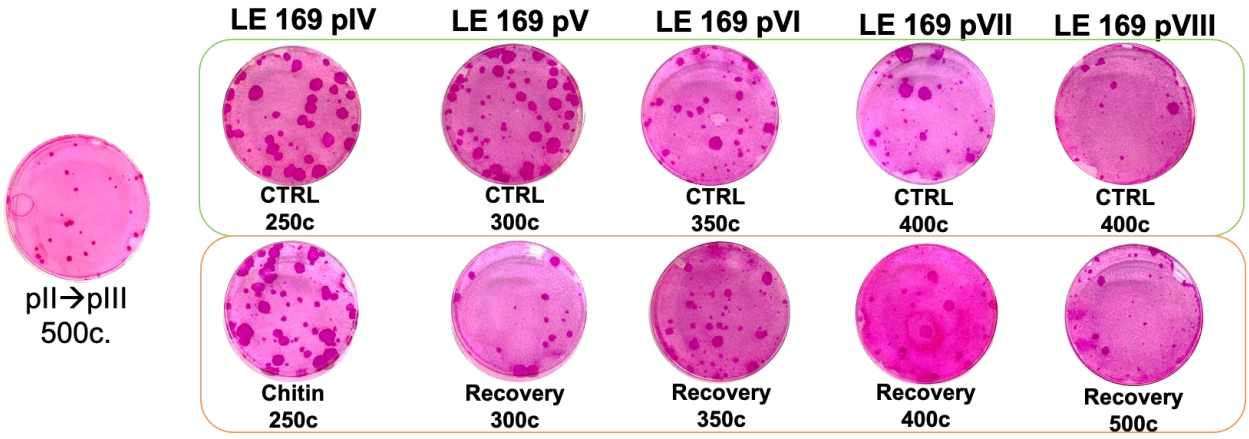

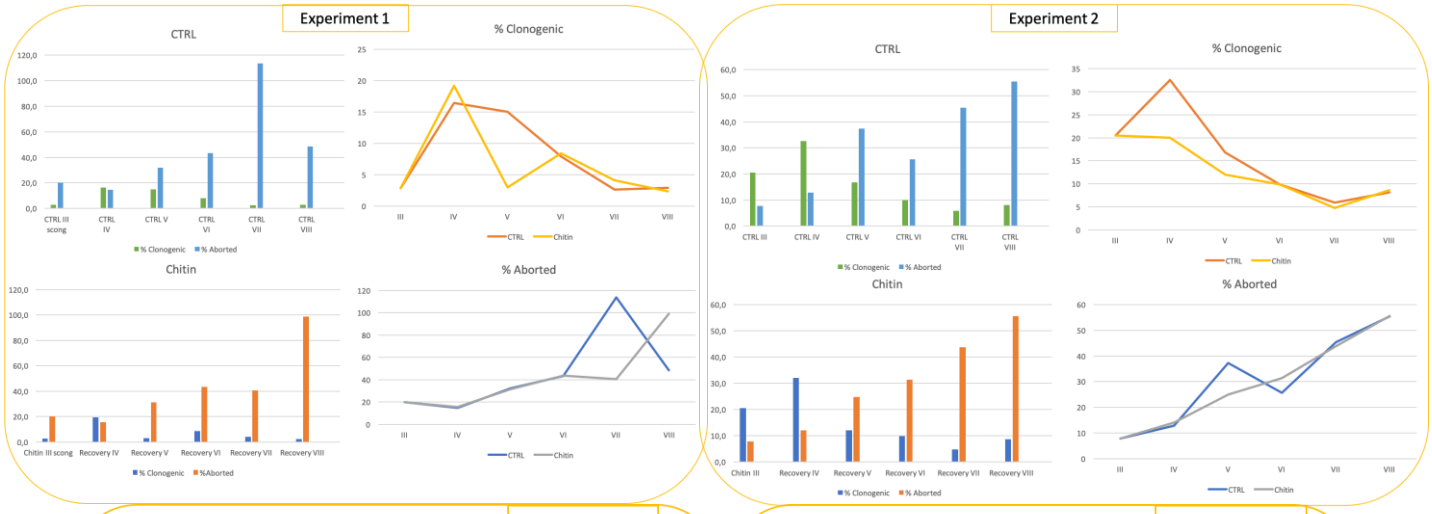

B

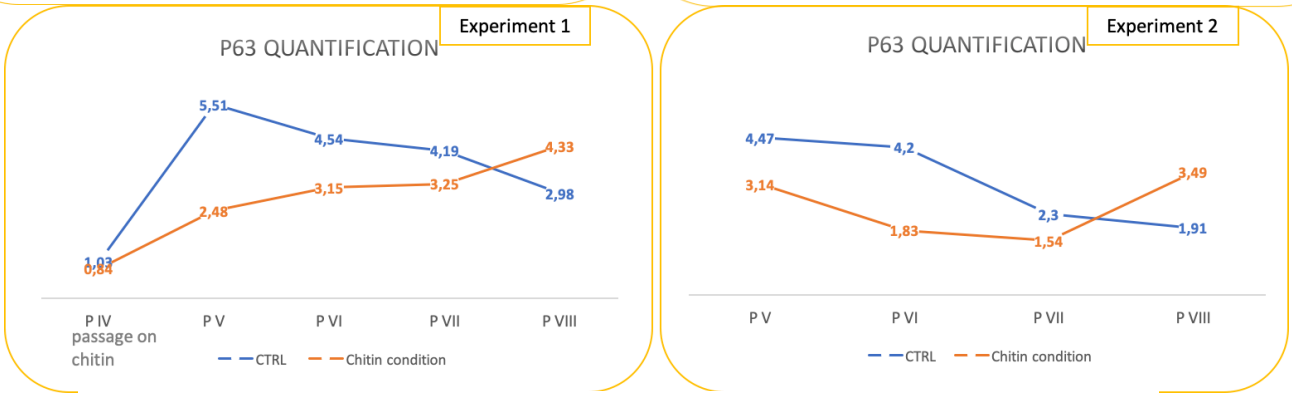

C

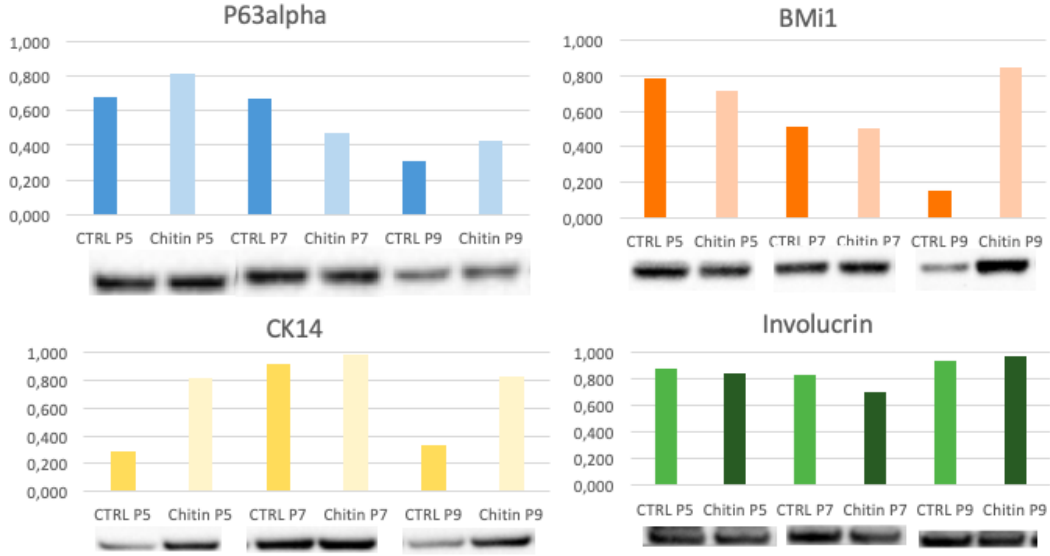

* All markers normalized by GAPDH

Figure 21 (A) Representative pictures of Colony Forming Efficiency analysis of two strain tested (B) p63α quantification of two strain tested: the percentage of p63 positive cells on the chitin scaffold condition seemed comparable to the control condition on plastic (C) western blot analysis: protein bands of cell identity marker (CK14), early epithelial differentiation marker (involucrin), stem/progenitor cells markers (p63α; BMI-1), and F/L contamination (vimentin).

DMAA scaffold and AcOH scaffold: functionalization with laminin 5

Alongside, to find the ideal scaffold for epithelial cells adhesion and growth, we changed the approach by (1) dispersing β-chitin in a dimethylacetamide and lithium chloride solution, (2) β-chitin dispersion in acetic acid.

- The DMMA films were transparent and qualitatively with good mechanical resistance (Fig. 22). The absorption spectrum of the film in water did not show visible peaks, and scattering was minimal. In Figure 22 C is shown an FTIR spectrum of a film obtained in DMAA/LiCl. Looking at the diagnostic peak around 1650 $cm^{-1,}$ it is possible to define that the polymorph is of α-chitin. When a single peak is present, it is diagnostic for β-chitin; whether this peak appears to split into two peaks it is α-chitin. Also, in figure 22, D is presented a UV-vis spectrum of a film obtained in DMAA/LiCl in water. There are no significant scattering or absorption peaks in the visible range. The UV spectrum is helpful to define that the squid pen has been completely deproteinized and, therefore, we do not observe any absorption, due to aromatic amino acids, at 280nm.

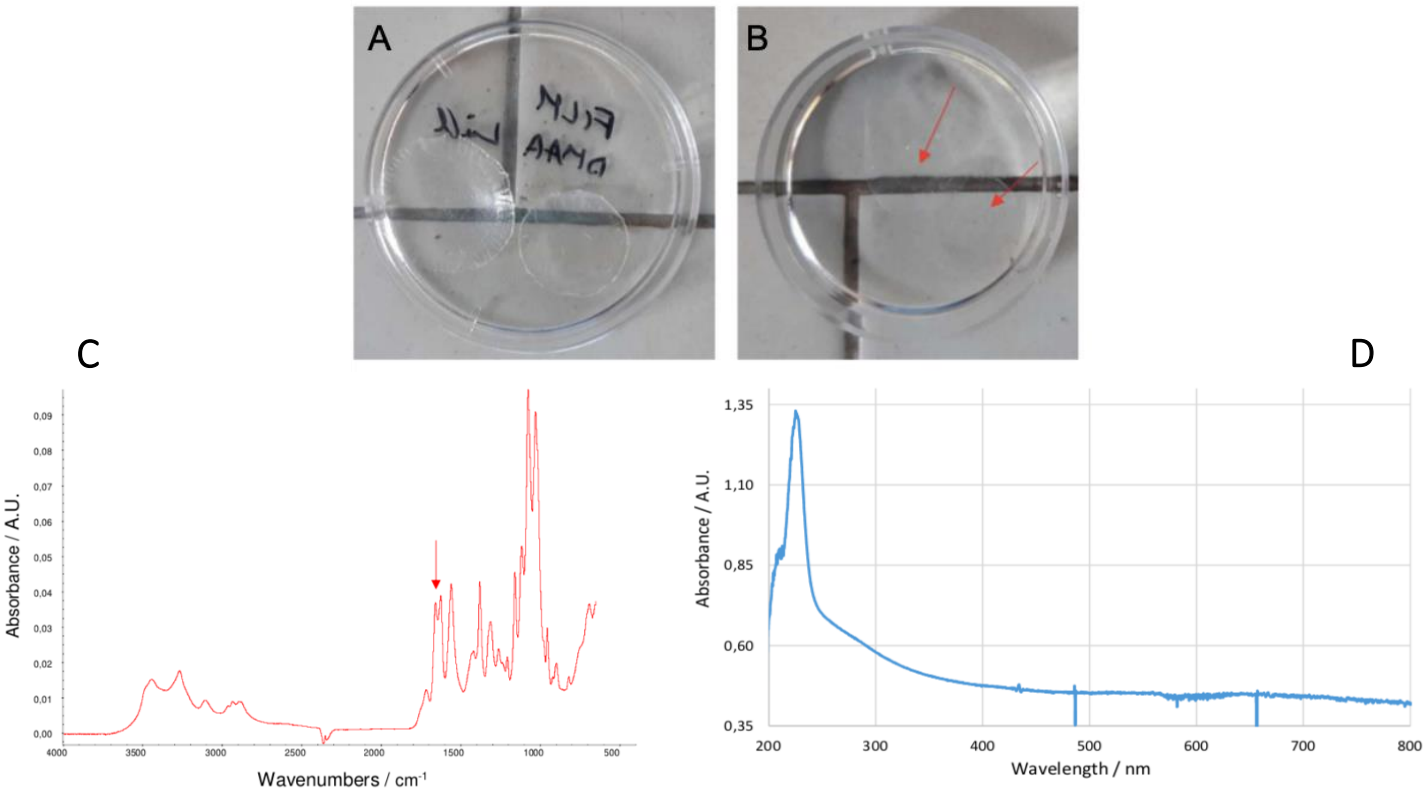

Fig. 22 Pictures of two films DMAA/LiCl obtained film dry (A) and in water (B). (C) FTIR spectrum of the dry films and (D) UV-vis spectrum of the wet films.

- For the AcOH scaffold, four samples were examined:

- two obtained by depositing 0.4 mL of each of the two dispersions obtained in a 24-well multiwell;
- two obtained by depositing 0.7 and 1.0 mL of the dispersion obtained by blender.

The first two samples were examined to evaluate the chitin obtained by the two methods; the other samples were to define the influence of the film thickness.

The dry films were transparent/whitish (fig. 23 A), and by FTIR (fig. 23 B) it was possible to confirm the β-chitin polymorph, as in the native pen. The FTIR spectrum reported was obtained from the sample prepared using the blender and successive deposition of 1 mL.

Then, the films were hydrated, and their absorption spectrum in water and swelling was measured. No absorption peak was detected in the UV spectrum (fig. 23 B), although an increase in the baseline was noted due to scattering, which explains the opalescence of the films. As it can be observed, the film obtained by stirring has a greater scattering.

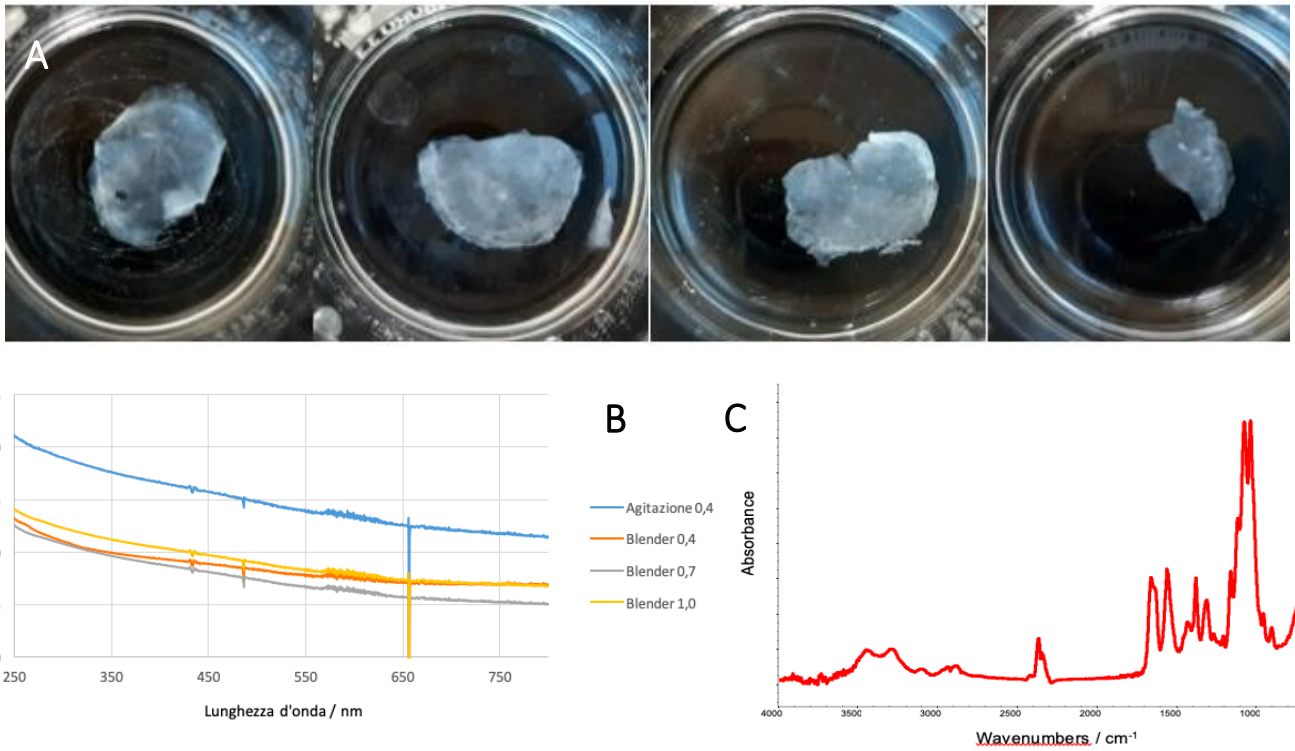

Fig. 23 (A) Pictures of the hydrated films on a black background. From left: film obtained by shaking and deposition of 0.4 mL, and films obtained by blender and depositing 1.0, 0.7 and 0.4 mL of gel. (B) UV-Vis spectrum of the film; (C) FTIR spectrum.

Comparing the two conditions, the AcOH film was opaque and lost its biomechanical characteristics, while the DMAA/LiCl film was more transparent and clear, maintaining its specifics. Thus, the DMAA/LiCl film has been selected for cell culture experiments.

To test the DMAA/LiCl film, the sterilization step in UV light for 1 hour was performed, followed by adding 5 µg/ml of laminin 332 to the DMAA/LiCl film; then, F/L cells and keratinocytes were seeded. This condition was compared to a control condition on plastic and a control condition on DMAA/LiCl film only (no addition of exogenous laminin 5).

As shown in figure 24, on day six of the culture, the condition of DMAA coated with laminin 5 appeared to be better than the control condition on DMAA/LiCl without the functionalization. However, the selected condition was still not ideal for keratinocytes growth. In conclusion, we can assume that cell attachment and growth existed, but the cell adhesion was still not homogeneous.

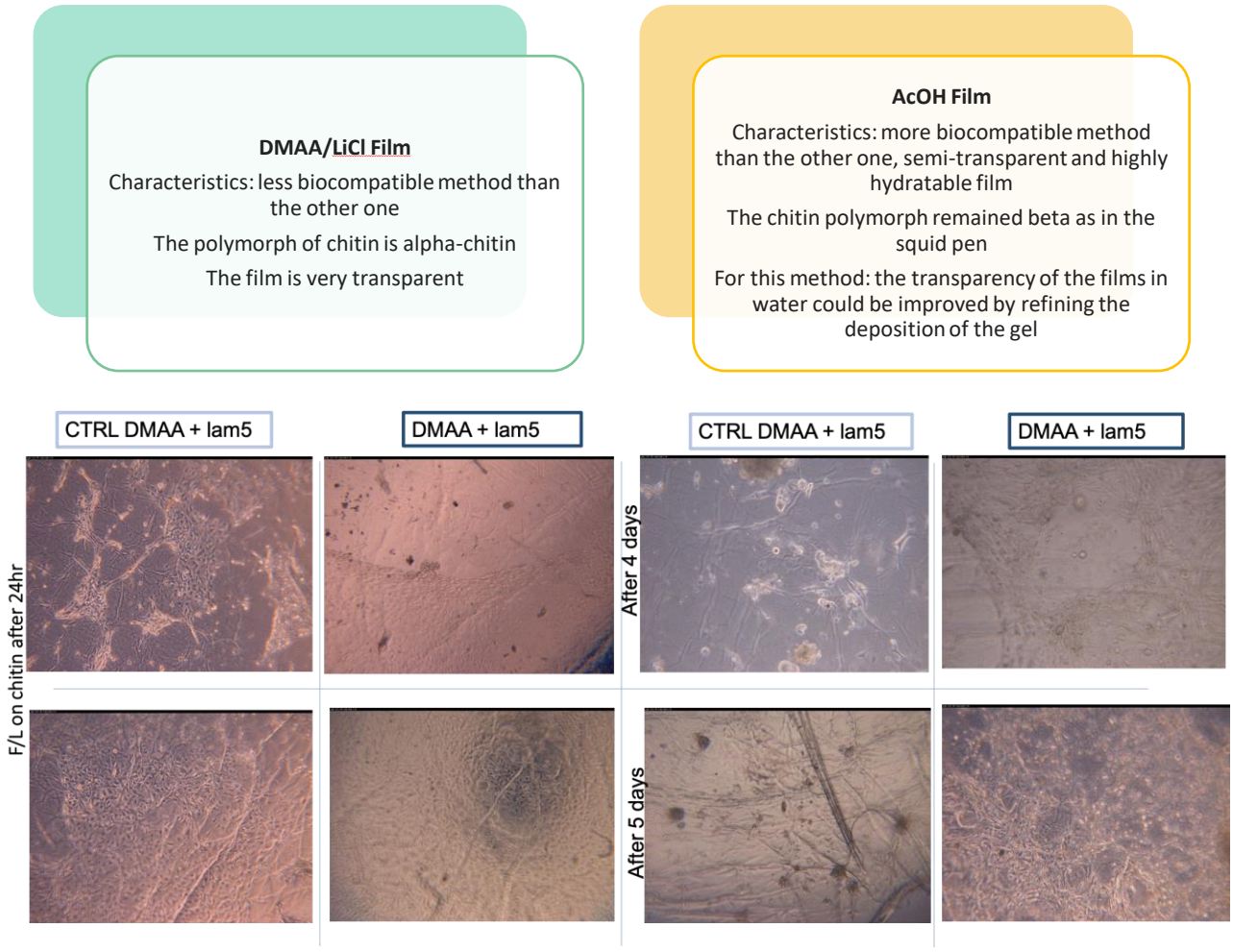

Fig. 24 Comparison between the DMAA/LiCl film and the control condition on plastic; after 24 hours and after four and five days of culture.

For this reason, due to the main problems occurred, we re-considered the original polymer, which represents the advantage of having correctly spaced *lamellae* that reproduce the corneal structure. Relying on this, we used the native structure of the squid pen, functionalizing it with an RGD peptide sequence.

Briefly, from here on, different possible approaches have been considered: (1) the squid pen coated with the RGD peptide, crucial to mediate cell attachment, and (2) the collagen-like biomaterials produced with entirely different types of polymers. This last option has been performed by collaborating with a Canadian laboratory directed by Prof. Griffith.

Chitin scaffold: functionalization with RGD tripeptide

As previously described, the tripeptide motif arginine – glycine – aspartate (RGD) is fundamental to mediate cell attachment. Proteins that contain the Arg-Gly-Asp (RGD) attachment site, together with the integrins that serve as receptors for them, constitute a significant recognition system for cell adhesion. Thus, in collaboration with the Chemistry Department "Giacomo Ciamician" of the University of Bologna, Italy, the β-chitin scaffold had been functionalized with the RGD sequence. For these experiments, we utilized deproteinized squid pens with a degree of acetylation around 75%, on which a decapeptide containing the RGDs sequence (H-RGDSGCWAWA-OH) has been linked to the free amines of chitin.

Short peptides are worthwhile compared to the whole protein since the protein tends to be randomly folded, and the receptor-binding domains are not always sterically available. Additionally, the short peptide is reasonably more stable during the modification process and can be massively synthesized in the laboratory.

The use of lectins and RGD sequence

These tests are realized binding the RGD peptide to the squid pen using lectins. In literature [82], many lectins of plant origin can bind chitin selectively. The chitin (in solid form) is immersed in a solution containing lectins (to be used instead of laminin 5) to distribute them uniformly on the surface. Thus, the lectins should bind firmly to the substrate. Conditions tested:

-chitin without RGD sequence or lectins (scaffold control condition)

-chitin linked to Wheat Germ Agglutinin (WGA) control condition: the pen on which the lectin adheres, but there is no RGD sequence

-a chitin condition where the RGD is linked to the WGA (already adhered to chitin) using a 1:5 *ratio* of coupling reagents

-a condition where the RGD is linked to the WGA (already adhered to chitin) and the coupling of the *ratio* of the reagents was 1:50 on chitin

The conditions were kept in culture for five days in total. Although, even if the cell attachment was visible, adhesion was not homogeneous and varied through conditions (fig. 25). Further analysis should be performed, and the condition implemented, finding the right quantity of WGA needed for the correct epithelial cell adhesion and growth.

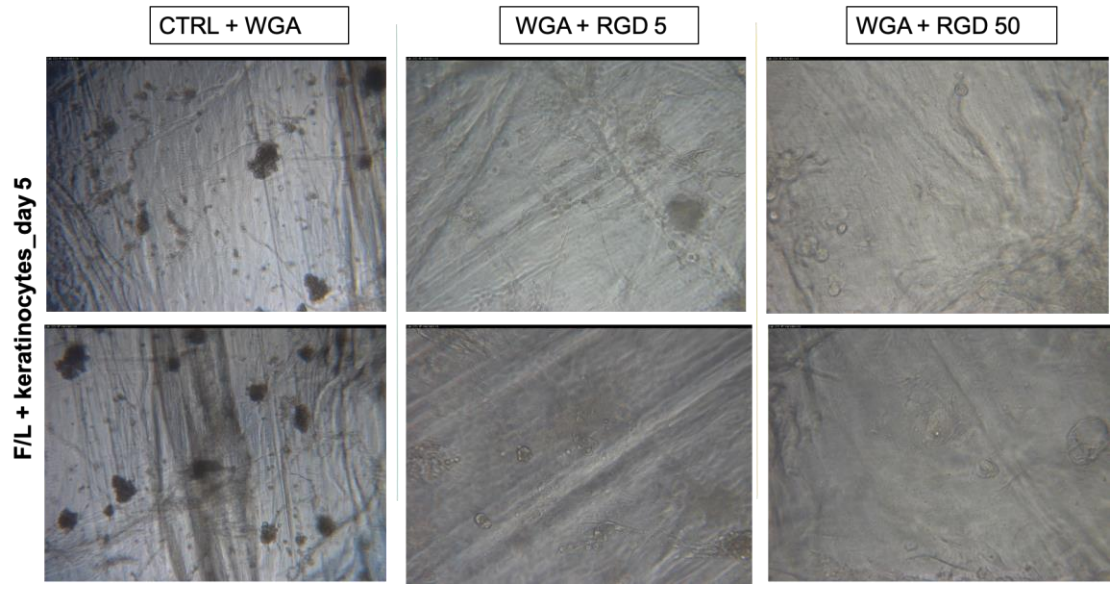

Fig. 25 From left: control without RGD sequence; condition with RGD sequence 1:5 *ratio* of reagents; condition with RGD sequence 1:50 *ratio* of reagents

The squid pen functionalized with RGD sequence only

The decapeptide has been designed and synthesized considering essential factors, such as the possibility of detecting the peptide in the chitin condition, the chance of quantifying it, and maximizing cellular adhesion. Six amino acids were inserted before the RGDs fragment; this step was crucial for improving the distance of the biologically active portion from the chitin matrix, making it more accessible to cells.

In this series of experiments, we firstly understood which percentage of RGD was ideal for cell adhesion and growth. Thus, we first seeded primary human keratinocytes on a treated 3% RGD-scaffold. The condition comprises an RGD peptide linked to the scaffold with a single coupling reaction (3%). However, low adhesion of keratinocytes on the treated material was observed. Thus, we proceeded to test the chitin scaffold with a double coupling reaction (4%), increasing the functionalization of the chitin pen with an RGD from 3% (single coupling) to 4% (double coupling). In the latter, full homogeneous coverage was observed (fig. 26).

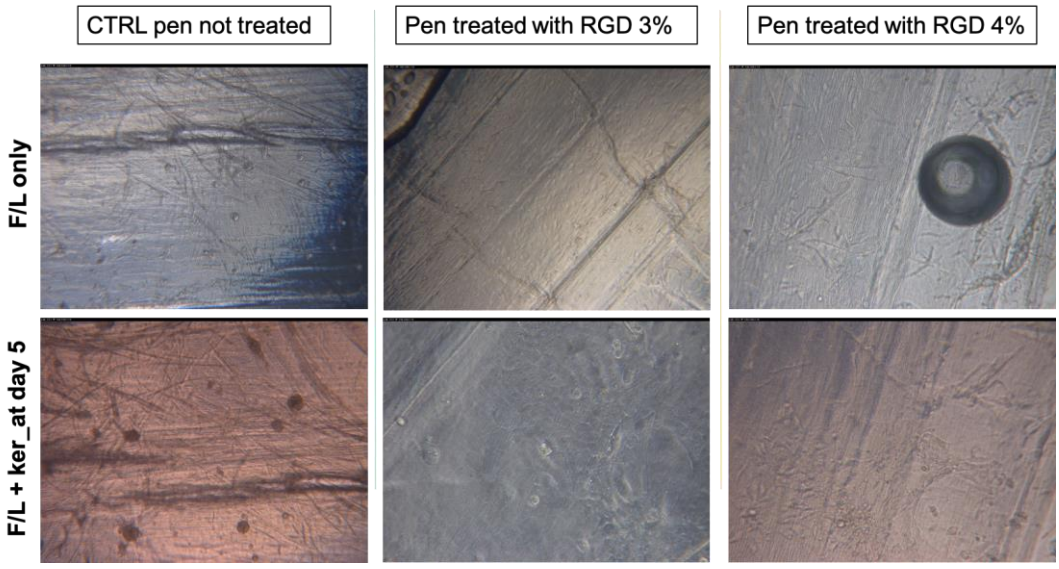

Fig. 26 Cell culture on different RGD functionalized scaffold. At day five of culture the condition with RGD 4% represent the best condition.

Standardization procedures for optimal squid pen cell seeding

Moreover, to reduce the "natural" variability that occurred in different squid pen dimensions and thicknesses, it was crucial to identify some standardization steps essential for future *in vitro* drug testing and possible clinical applications. In several analyses, we considered some values such as the number of coupling performed on the squid pen, the length and width of the pen, the area, and the thickness of the whole pen (fig. 27). Finally, we concluded that the squid pen with a dimension < 15cm and a double coupling reaction represented the best condition for cell adhesion and growth (data not shown). Hereafter, the experiments were all performed keeping into consideration this standardized condition.

Pen	Position	N° coupling	Mass (mg)	Width (mm)	Length (mm)	Surface (mm^2)	Mass/surface (mg/mm^2)	Thickness (mm)	B λ 456 nm (T%)	G λ 546 nm (T%)	R λ 700 nm (T%)
A1	Far from the rib	1	5,91	8	9	72 ± 17	0,08 ± 0,02	0,19 ± 0,03	60 ± 15	65 ± 15	67 ± 14
A2	Near the rib	1	5,63	7	9	63 ± 16	0,09 ± 0,02	0,21 ± 0,06	35 ± 6	39 ± 6	40 ± 7
B1	Near the top	1	4,48	8	7	56 ± 15	0,08 ± 0,02	0,23 ± 0,01	36 ± 19	39 ± 20	40 ± 21
B	Center	1	5,7	8	8	64 ± 16	0,09 ± 0,02	0,24 ± 0,14	57 ± 13	61 ± 13	64 ± 12
BB	Center	2	5,08	7	8	56 ± 15	0,09 ± 0,02	0,26 ± 0,02	64 ± 13	67 ± 13	70 ± 14
B2	Near the low tip	1	3,52	8	7	56 ± 15	0,06 ± 0,02	0,28 ± 0,02	67 ± 9	69 ± 10	70 ± 11
C	Center	1	3,59	7	7	49 ± 14	0,07 ± 0,02	0,24 ± 0,04	49,2 ± 0,8	54,5 ± 0,2	58,31 ± 0,05
CC	Center	2	3,09	6	8	48 ± 14	0,06 ± 0,02	0,19 ± 0,03	51 ± 13	55 ± 14	58 ± 15
Cntrl	-	0	8,11	7	8	56 ± 15	0,14 ± 0,04		9 ±	11 ±	11 ±
Cntrl	-	0	5,62	6	6	36 ± 12	0,16 ± 0,05		37 ±	41 ±	41 ±

Squid pen used	L (cm)	l (cm)
A	21,5	2,0
B	18,0	1,5
C	15,5	1,0

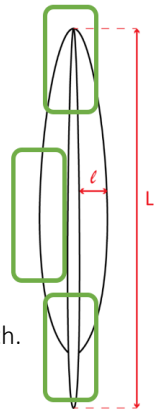

Fig. 27 Analysis performed for standardization procedures.

The blue arrows represent which squid pen was ideal for cell growth.

RGD chitin scaffold biocompatibility tests

After confirming the suitability of the condition with double coupling of RGD and with the length of the pen <15cm was suitable for cell adhesion, a serial cultivation assay was performed to verify the maintenance of stem cells content on a long-term contact with the scaffold. Serial passages of culture on the material supported the evaluation of acute and chronic toxicity (fig. 28 and 29).

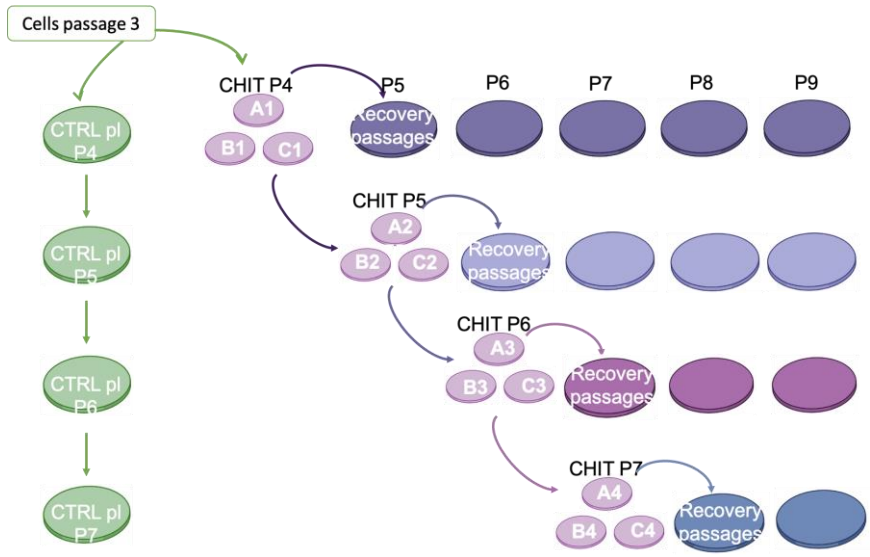

Fig 28. Scheme of the RGD serial cultivation experiment. Four passages of cell culture on the chitin condition were conducted. In parallel, four passages of the control condition were performed. Several recovery passages on plastic were carried out from each chitin passage to understand if acute or chronic toxicity occurred.

A

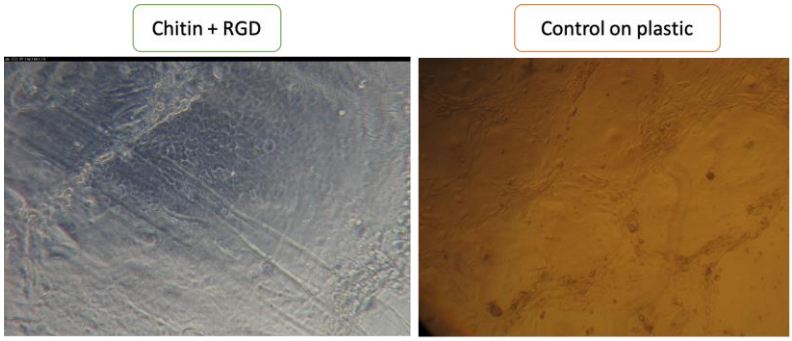
Chitin + RGD
Control on plastic

B

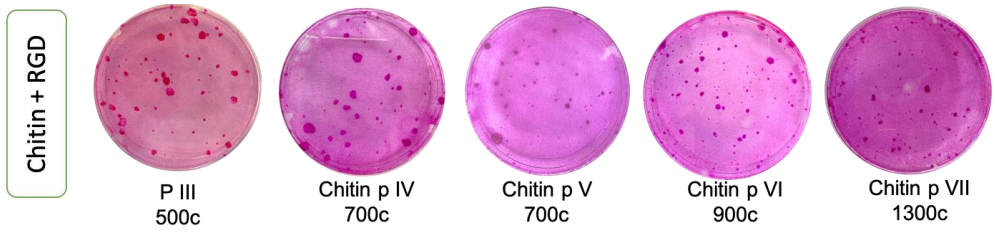
Chitin + RGD
P III
500c
Chitin p IV
700c
Chitin p V
700c
Chitin p VI
900c
Chitin p VII
1300c

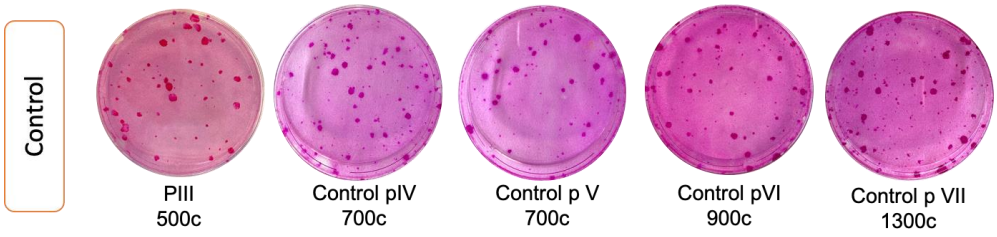
Control
PIII
500c
Control pIV
700c
Control p V
700c
Control pVI
900c
Control p VII
1300c

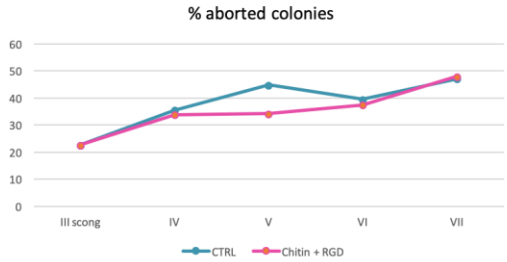
% aborted colonies
60
50
40
30
20
10
0
III scong
IV
V
VI
VII
CTRL
Chitin + RGD

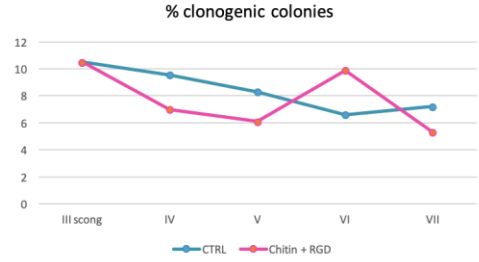
% clonogenic colonies
12
10
8
6
4
2
0
III scong
IV
V
VI
VII
CTRL
Chitin + RGD

C

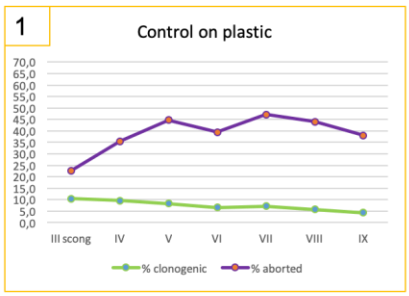
1
Control on plastic
III scong
IV
V
VI
VII
VIII
IX
% clonogenic
% aborted

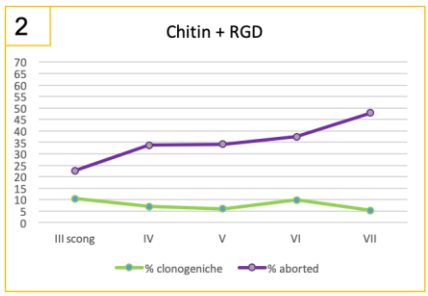
2
Chitin + RGD
III scong
IV
V
VI
VII
% clonogeniche
% aborted

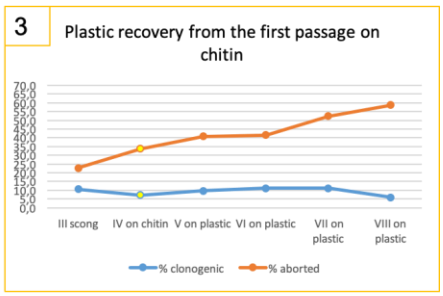
3
Plastic recovery from the first passage on chitin
III scong
IV on chitin
V on plastic
VI on plastic
VII on plastic
VIII on plastic
% clonogenic
% aborted

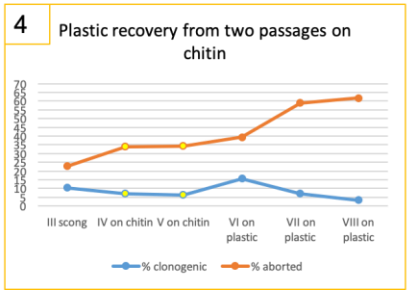
4
Plastic recovery from two passages on chitin
III scong
IV on chitin
V on chitin
VI on plastic
VII on plastic
VIII on plastic
% clonogenic
% aborted

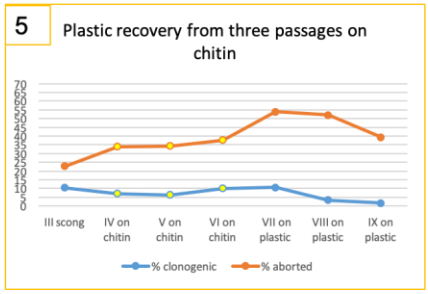
5
Plastic recovery from three passages on chitin
III scong
IV on chitin
V on chitin
VI on chitin
VII on plastic
VIII on plastic
IX on plastic
% clonogenic
% aborted

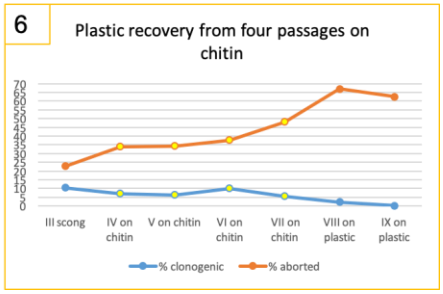
6
Plastic recovery from four passages on chitin
III scong
IV on chitin
V on chitin
VI on chitin
VII on chitin
VIII on plastic
IX on plastic
% clonogenic
% aborted

Fig. 29 Biocompatibility tests: assessment of the possible acute and chronic epithelial cytotoxicity on the scaffold. (A) comparable results for both CTRL and the condition on chitin (B) graphical representation of the CFE assessment for each passage on plastic (CTRL culture) and on several passages on chitin. As shown by the percentage of clonogenic cells (blue lines) and aborted colonies (pink lines), the cells on the material had the same behavior of the ones on plastic; (C) no acute toxicity (C3) or chronic toxicity (C4-C5-C6) occurred in all conditions tested.

Specifically, F/L and keratinocyte cells were seeded onto the chitin scaffold and cultured for five days as previously described to evaluate possible acute toxicity. Then, the epithelial cells were enzymatically detached by the scaffold, and CFE analysis was performed. The remaining cells were serially sub-cultivated for additional passages in standard culture conditions on plastic to evaluate the extent of cell recovery in case acute toxicity occurred. The keratinocytes were serially cultivated onto the scaffold to assess the chronic toxicity. Specifically, the keratinocytes detached from one RGD-scaffold (pIII) were re-plated onto a new RGD-scaffold (PIV) and so on up to pVII. Thus, this operation was repeated for four consecutive passages to evaluate the effect of extended contact and growth of the epithelial cells onto the scaffold surface (fig. 29 C4-6). Indeed, this prolonged contact can *in vitro* simulate the *in vivo* regeneration of the tissue over time. Also, serial passages in standard culture conditions on plastic have been used as a control for acute and chronic toxicity assessment.

Subsequently, as presented in figure 29, no acute or chronic cytotoxicity was detected in the cultures grown for one passage or for four consecutive passages onto the selected RGD-scaffold. Moreover, the percentage of clonogenic cells after one passage (p III) ad up to four successive passages of culture onto the scaffold (p VII) was high for both the chitin and the standard culture condition. At the same time, the percentage of aborted colonies at the end of the four passages was comparable for the chitin and the standard culture condition. These *in vitro* tests proved the absence of acute or chronic epithelial cell cytotoxicity and the suitability of the selected 3D scaffold for cell adhesion and proliferation.

To complete the analysis, the percentage of p63α positive cells that underpins epithelial stem cells' proliferative, regenerative capacity was considered. The percentage of p63α positive cells collected from different passages of the RGD-scaffold, appeared to be comparable to the control on plastic, confirming previous data (fig. 30 A).

Immunofluorescence analysis on frozen sections of the 3D construct confirmed the ability of the corneal epithelial cells to adhere to the scaffold surface efficiently. These cells retained their basal epithelial nature (as highlighted by the CK14 expression), and they correctly expressed 14-3-3σ, an early differentiation marker, result comparable to the control condition on plastic. Moreover, they proliferated, giving rise to a continuous monolayer of basal cells lining the scaffold surface, as visible in figure 30 B.

A

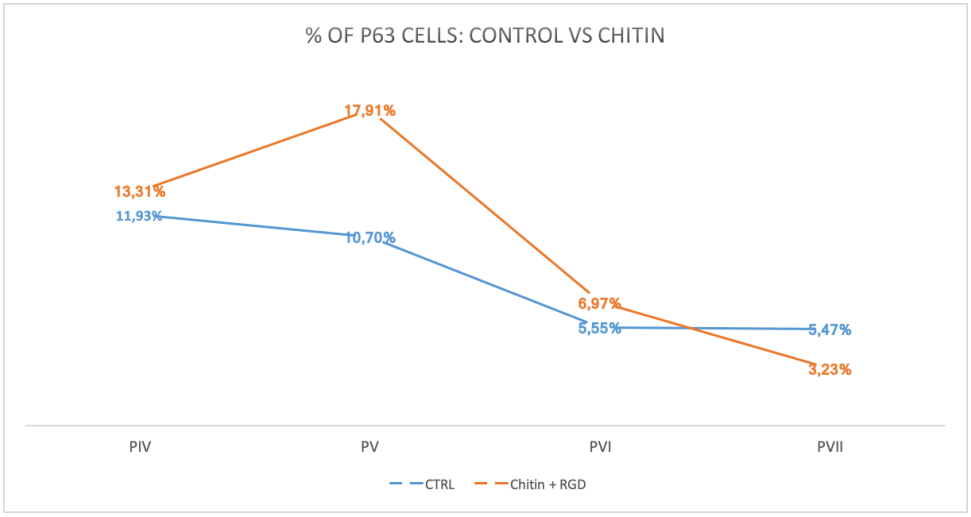

B

Squid Pen

CTRL on plastic

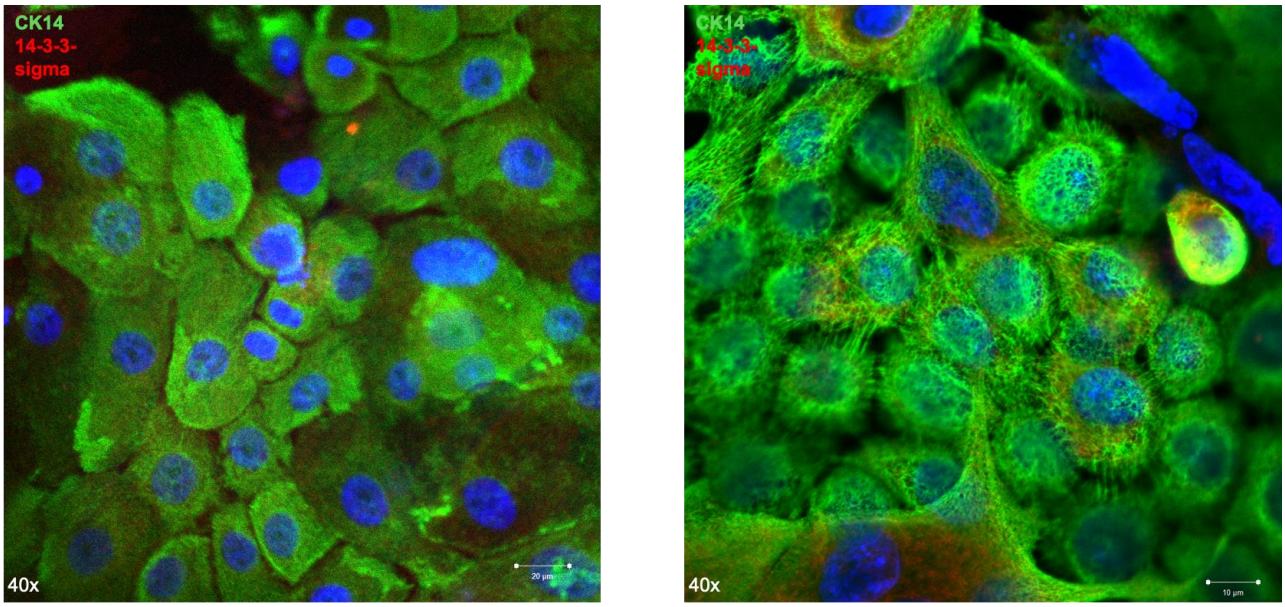

Fig. 30 (A) The percentage of p63α positive cells of the chitin condition was comparable to the control sample. (B) Immunofluorescence analysis of CK14 expression, a specific marker of epithelial basal cells, and 14-3-3σ, an early differentiation marker.

Collagen-like biomaterials

In collaboration with the Tissue Engineering laboratory of Professor Griffith, in Montreal, Canada, we tested human corneal epithelial cell line onto the selected scaffolds to understand their biocompatibility with epithelial cells and the possible acute toxicity the scaffolds had on the selected cell type.

CLP-PEG and CLP-PEG MPC scaffolds

After sterilization with Chloroform 1% performed O/N, the scaffolds were rinsed in PBS1x for 3-4 days and then HCEC cell type was seeded and cultured as explained for four days onto both hydrogels and the control on plastic. We considered the condition on plastic and the CLP-PEG hydrogel as our controls and the CLP-PEG-MPC scaffold as our condition to examine.

To ensure that the selected hydrogels supported cell differentiation, HCECs were cultured on 5 mm discs of hydrogels in a 96 well plate. The cells were maintained in KSFM medium for four days. Cells were able to grow properly on both hydrogels being able to cover completely the surface (fig. 31). To complete the evaluation, the cells were fixed with 4% paraformaldehyde and stained with cytokeratin 3, a differentiation marker for corneal epithelium-specific protein (fig. 32). Future experiments will include *in vitro* tests with human primary keratinocytes, to validate their growth on the selected hydrogels.

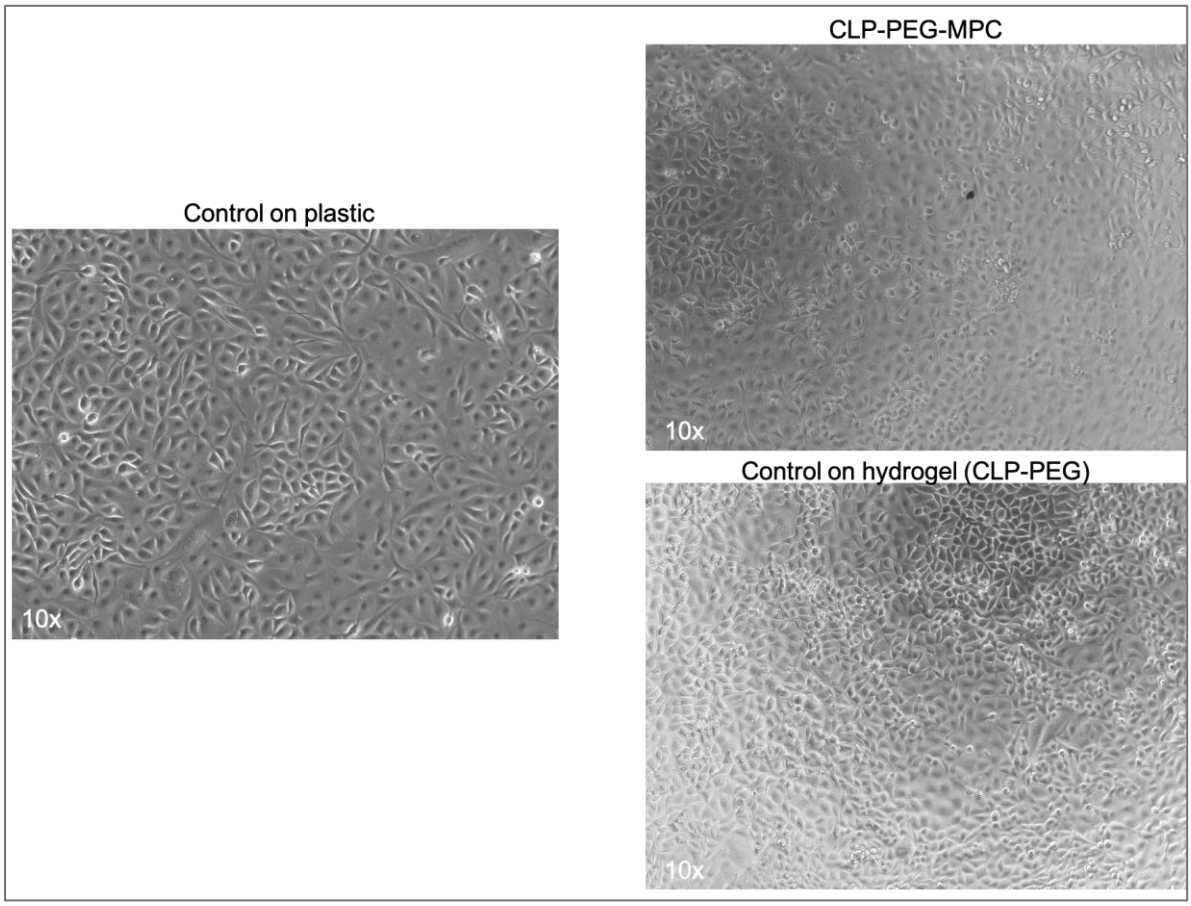

Fig. 31 HCEC line on control samples (culture on plastic and control on CLP-PEG hydrogel) and hydrogel sample CLP-PEG-MPC.

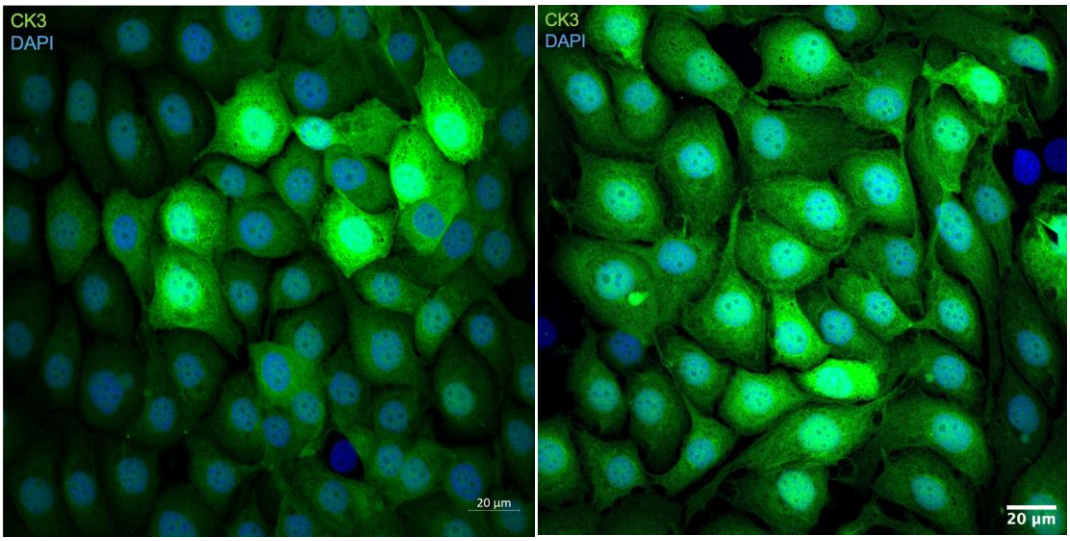

Fig. 32 On the left: Cytokeratin 3 staining of control on CLP-PEG. On the right: CLP-PEG MPC hydrogel.

Discussion

The vision is the most prevalent of our senses, and the universal need for eye care is going to increase drastically in the upcoming decades, presenting a considerable challenge for health system organizations.

In fact, according to WHO, blindness is defined as visual acuity of 3/60 or less, and diseases affecting the cornea represent the leading cause of blindness globally, second only to cataracts in real relevance [1]. The epidemiology of corneal blindness is of global interest and includes a range of inflammatory and infectious eye diseases that provoke corneal scarring. Also, the incidence of corneal disease differs from one country and from one population of individuals to another.

To date, on the world stage, more than 2.2 billion individuals have blindness or visual impairment, and of these, about 1 billion have a vision impairment that could have been avoided or has yet to be treated [83]. Preventing vision impairment and eye conditions will guide to improved productivity and reduce informal and intangible costs [2].

On the other side, tissue engineering has become a promising option to address critical medical needs. TE and regenerative medicine are multidisciplinary fields that merge the technologies and knowledge from different areas such as engineering, biology, chemistry, pharmaceutical, medicine, and material science to develop products and therapies for the replacement or repair of damaged tissues and organs [84].

Corneal TE approaches are crucial to maintain the transparent interface between the eye and the environment of the cornea in case of corneal damage occurs. The cornea comprises three main layers: the epithelium, the stroma, and the endothelium, and, between those, the most difficult to replace is represented by the stroma.

So far, corneal transplantation is the main used surgical procedure in case the damage comprises the stroma. The latter can be replaced entirely by donor corneas (PK procedure) or in part (lamellar keratoplasty). As previously discussed, these procedures bring to main problems such as graft rejection, donor corneas shortage, and risks of infection [85]. Several studies have been presented; however, successful *in vitro* and *in vivo* data and clinical applications are still lacking.

Instead, the biomaterial is considered a microenvironment for cell seeding survival and the key for corneal TE reconstruction. The scaffold should be (i) a temporary support, determining the contour to repair the cornea, (ii) a carrier for adhesion and proliferation of corneal cells, guiding proliferation and growth of cells that are seeded onto the scaffold. Thus, (iii) it should provide the basis for cell adhesion, migration, proliferation, and differentiation [86].

Thus, considering that the ideal TE corneal scaffold must have excellent optical characteristics such as biocompatibility, biodegradability, biomechanical strength, and mechanical properties, we decided to test different scaffolds that reflect these essential specifics.

In particular, the β-chitin scaffold was considered for its high transparency offering interesting parameters essential to guarantee hemi-corneal reconstruction. This scaffold displays excellent features such as outstanding biocompatibility and biodegradability. Mainly, this material has high stiffness and significant biomechanical strength.

Secondly, the collagen-like peptide (CLP) scaffolds were considered for corneal reconstruction when conjugated to polyethylene glycol (PEG) and inflammation-suppressing polymeric 2-methacryloyloxyethyl phosphorylcholine (MPC), resulting in the CLP-PEG MPC hydrogel. In previous studies, compared to the CLP-PEG-only hydrogels, these hydrogels appeared to be at a more advanced regeneration stage when grafted into a mini-pig cornea alkali burn model of inflammation over 12 months [75, 87]. However, *in vitro* test analysis to perform scaffold suitability for humans still needed to be conducted.

We aimed at developing scaffolds that accurately mimic the ECM biologically and mechanically. Specifically, we considered scaffolds able to re-create the extracellular environment.

For this reason, in the present manuscript, we first proposed the immobilization of collagen IV and fibronectin (a protein containing several cell-binding domains) on a chitin substrate. However, although collagen IV and fibronectin play an essential role in keratinocytes' adhesion and proliferation, the functionalized β-chitin scaffold was not ideal for cell adhesion and proliferation. The cell adhesion on the scaffold was discontinuous and not homogeneous. CFE analysis revealed a decrease in clonogenic colonies and an increase in aborted colonies in the scaffold treated condition compared to the control on plastic, resulting in an early clonal conversion of cell cultures cultured on the scaffold compared to the condition on plastic.

In addition, the use of aptamers was interesting for cell binding and growth onto the selected β-chitin scaffold. The promising innovation of aptamers brought us to identify them to specifically enrich the biomaterial with specific molecules naturally occurring in damaged tissues and involved in the regeneration process: laminin and fibronectin.

Looking up to the results obtained using aptamers screened against fibronectin and human exogenous fibronectin functionalization, the cells seeded onto the treated chitin scaffold had comparable results with the control culture condition on plastic. To increase the cell adhesion, we proposed to modify fibronectin adsorption by adding aptamers selected against this protein, with an SH-group on their 3′ end. The cells were able to grow correctly on the functionalized scaffold for one passage, and the results showed no acute toxicity for cells grown on the scaffold. Also, recovery passages of cells grown on scaffold seemed to be similar to those grown on plastic, suggesting that our scaffold did not cause any irreversible damage to keratinocytes viability.

These results were confirmed by CFE analysis, western blot analysis, and p63α quantification. The *in vitro* expression and localization of critical epithelial markers were qualitatively (IF) and quantitatively (WB) assessed along the passages of the cultures. The basal markers (CK14), the early epithelial differentiation markers (Involucrin and 14-3-3 sigma), and the stem/progenitor cell markers (p63α

and BMI-1) proved the ability of the culture system to support the basal cell long-term proliferation without altering their ability to differentiate.

However, variability in the scaffold starting material was observed despite the excellent adhesion and proliferation of keratinocyte cell type.

Thus, an important feature that was thereafter considered in our experiments was the standardization of the starting biomaterial. The chitin scaffold, derived from *Loligo Vulgaris* native pen, is a natural biomaterial and usually a waste product of fishing industries. Since its natural origin and variability between *gladii*, for our group, it was mandatory to reduce the variability that occurred in different squid pen dimensions and thickness by analyzing the length and width of the pen, the area, and the thickness. As presented in the results section, the squid pen with < 15cm dimension was suitable for cell adhesion and growth. Hereafter, the experiments were all performed, considering this standardized condition.

Thus, to improve cell adhesion, small peptide fragments containing integrin-binding domain (i.e., RGD arginine-glycine-aspartate peptide) were immobilized on scaffold surfaces. These small bioactive molecules promote cell adhesion and the assembly of several ECM proteins, including fibronectin, laminin, various collagen isoforms, and many other molecules [88, 89].

The preliminary results obtained by scaffold functionalization with 4% of RGD sequence proved the scaffold's biocompatibility with the corneal epithelial cells, as they efficiently adhered and proliferated onto its surface without acute (one passage on chitin) or chronic cytotoxicity (up to four serial passages on chitin). Thus, IF, CFE analysis, and p63α quantification were assessed along the serial passages of the cultures on the selected scaffold and then compared with the control condition on plastic. We observed the correct expression and localization of the epithelial stem cells markers and the early differentiation markers in cells grown on the selected scaffold compared to the control condition on plastic as shown by IF analysis. Additional proliferation markers, such as ki67, and adhesion markers, such as integrin α6, will be analyzed in future experiments. In conclusion, cells preserved their epithelial nature and the expression of the epithelial stem cell markers.

Taken together, our results highlight the ability of a proper binding of RGD peptide to maintain epithelial cells behavior on chitin substrate, and future analysis will be necessary to replicate those consistent data. These preliminary data support the idea that the functionalized scaffold maintain the proliferation and the correct differentiation of corneal epithelial cells *in vitro*, showing good biocompatibility.

Furthermore, safety and efficacy parameters must be considered in cell cultures for clinical purposes in the expansion procedure. Long-term cultures must assess the absence of alterations in cellular physiology and immortalization events.

Also, the continuous process of standardization will be fundamental and critical for future clinical purposes. The maintenance of high standards is crucial in securing the results' credibility, reproducibility, acceptance, and application.

Concerning the DMAA/LiCl films, human primary cells seeding was not optimal compared to other conditions. Cells could not grow uniformly onto the scaffold surface and maintain their shape onto the selected material, compared to the control condition on plastic. However, the material was highly transparent and resistant while in culture condition. Thus, more degradability tests should be performed, and several other experiments should be carried out to functionalize the examined material better.

Instead, the preliminary data produced on the *in vitro* characterization of the CLP-PEG MPC scaffolds were optimistic. It was essential to understand the possible acute toxicity of the material while seeding the HCEC line onto the selected scaffold. Based on our data, no type of acute toxicity occurred. The cell line tested had comparable cell size and shape compared to the control condition where the HCEC line was cultured on plastic. Future experiments will include human primary keratinocytes seeded onto the CLP-PEG (our control) and CLP-PEG MPC scaffold (our condition) to evaluate the *in vitro* biocompatibility of those cells with the material. Several studies will be performed, such as qualitatively (IF) and quantitatively (WB) tests. We would like to understand if, after different serial passages on scaffold condition, markers such as p63 and Bmi1 could seem comparable to those grown on plastic; this will confirm that our scaffold does not cause irreversible damage in keratinocytes viability and stemness. Crucial will be the investigation of other specific human keratinocyte markers by immunofluorescence analysis, which will further confirm the suitability of this scaffold.

Following the project development, the analyzed protocols for corneal restoration will further improve quality of life due to proven biocompatibility and longer duration of implants; patients won't need immunosuppression and could resume their everyday lives.

Soon in the project, we expect to characterize the proposed scaffolds properly. In the case of large-scale market deployment of this therapy, the use of fish leftovers could contribute to the setup of an environmentally friendly value chain.

Furthermore, the cornea has a high level of complexity; therefore, standardization of each step will be mandatory. We expect to produce an effective human model for clinical purposes, test new drugs and treatments, and investigate mechanisms of action without animal use, often producing misleading results.

Bibliography

1. Whitcher, J.P., M. Srinivasan, and M.P. Upadhyay, *Corneal blindness: a global perspective*. Bulletin of the world health organization, 2001. **79**: p. 214-221.
2. Magrelli, F.M., A. Merra, and G. Pellegrini, *Surgery Versus ATMPs: An Example From Ophthalmology*. Front Bioeng Biotechnol, 2020. **8**: p. 440.
3. Pellegrini, G., et al., *Long-term restoration of damaged corneal surfaces with autologous cultivated corneal epithelium*. Lancet, 1997. **349**(9057): p. 990-3.
4. Ianiro, A., et al., *Customizing properties of β-chitin in squid pen (gladius) by chemical treatments*. Mar Drugs, 2014. **12**(12): p. 5979-92.
5. Islam, M.M., et al., *Self-assembled collagen-like-peptide implants as alternatives to human donor corneal transplantation*. RSC advances, 2016. **6**(61): p. 55745-55749.
6. Thoft, R.A., J. Friend, and H.S. Murphy, *Ocular surface epithelium and corneal vascularization in rabbits. I. The role of wounding*. Investigative Ophthalmology & Visual Science, 1979. **18**(1): p. 85-92.
7. Kinoshita, S., et al., *Characteristics of the human ocular surface epithelium*. Progress in retinal and eye research, 2001. **20**(5): p. 639-673.
8. Gipson, I.K., *The ocular surface: the challenge to enable and protect vision: the Friedenwald lecture*. Investigative ophthalmology & visual science, 2007. **48**(10): p. 4391-4398.
9. Sridhar, M.S., *Anatomy of cornea and ocular surface*. Indian journal of ophthalmology, 2018. **66**(2): p. 190.
10. Rüfer, F., A. Schröder, and C. Erb, *White-to-white corneal diameter: normal values in healthy humans obtained with the Orbscan II topography system*. Cornea, 2005. **24**(3): p. 259-61.
11. Ruberti, J.W., A. Sinha Roy, and C.J. Roberts, *Corneal biomechanics and biomaterials*. Annu Rev Biomed Eng, 2011. **13**: p. 269-95.
12. Hancox, Z., et al., *The progress in corneal translational medicine*. Biomater Sci, 2020. **8**(23): p. 6469-6504.
13. DelMonte, D.W. and T. Kim, *Anatomy and physiology of the cornea*. J Cataract Refract Surg, 2011. **37**(3): p. 588-98.
14. Mantelli, F., J. Mauris, and P. Argüeso, *The ocular surface epithelial barrier and other mechanisms of mucosal protection: from allergy to infectious diseases*. Curr Opin Allergy Clin Immunol, 2013. **13**(5): p. 563-8.
15. McKay, T.B., et al., *Integrin: Basement membrane adhesion by corneal epithelial and endothelial cells*. Exp Eye Res, 2020. **198**: p. 108138.
16. Sridhar, M.S., *Anatomy of cornea and ocular surface*. Indian J Ophthalmol, 2018. **66**(2): p. 190-194.
17. Dua, H.S. and A. Azuara-Blanco, *Limbal stem cells of the corneal epithelium*. Surv Ophthalmol, 2000. **44**(5): p. 415-25.
18. Rama, P., et al., *Limbal stem-cell therapy and long-term corneal regeneration*. N Engl J Med, 2010. **363**(2): p. 147-55.

19. De Rosa, L., et al., *Laminin 332-Dependent YAP Dysregulation Depletes Epidermal Stem Cells in Junctional Epidermolysis Bullosa*. Cell Rep, 2019. **27**(7): p. 2036-2049.e6.

20. Lagali, N., J. Germundsson, and P. Fagerholm, *The role of Bowman's layer in corneal regeneration after phototherapeutic keratectomy: a prospective study using in vivo confocal microscopy*. Invest Ophthalmol Vis Sci, 2009. **50**(9): p. 4192-8.

21. Meek, K.M., *Corneal collagen-its role in maintaining corneal shape and transparency*. Biophys Rev, 2009. **1**(2): p. 83-93.

22. Meek, K.M. and C. Knupp, *Corneal structure and transparency*. Prog Retin Eye Res, 2015. **49**: p. 1-16.

23. Donohue, D.J., et al., *Numerical modeling of the cornea's lamellar structure and birefringence properties*. J Opt Soc Am A Opt Image Sci Vis, 1995. **12**(7): p. 1425-38.

24. Ghezzi, C.E., J. Rnjak-Kovacina, and D.L. Kaplan, *Corneal tissue engineering: recent advances and future perspectives*. Tissue Eng Part B Rev, 2015. **21**(3): p. 278-87.

25. Eghrari, A.O., S.A. Riazuddin, and J.D. Gottsch, *Overview of the Cornea: Structure, Function, and Development*. Prog Mol Biol Transl Sci, 2015. **134**: p. 7-23.

26. Barrandon, Y. and H. Green, *Three clonal types of keratinocyte with different capacities for multiplication*. Proc Natl Acad Sci U S A, 1987. **84**(8): p. 2302-6.

27. Pellegrini, G., et al., *Location and clonal analysis of stem cells and their differentiated progeny in the human ocular surface*. J Cell Biol, 1999. **145**(4): p. 769-82.

28. Barrandon, Y. *The epidermal stem cell: an overview*. in *Seminars in Developmental Biology*. 1993. Elsevier.

29. Hirsch, T., et al., *Regeneration of the entire human epidermis using transgenic stem cells*. Nature, 2017. **551**(7680): p. 327-332.

30. Di Iorio, E., et al., *Isoforms of DeltaNp63 and the migration of ocular limbal cells in human corneal regeneration*. Proc Natl Acad Sci U S A, 2005. **102**(27): p. 9523-8.

31. Pellegrini, G., et al., *p63 identifies keratinocyte stem cells*. Proc Natl Acad Sci U S A, 2001. **98**(6): p. 3156-61.

32. Pellegrini, G., et al., *Biological parameters determining the clinical outcome of autologous cultures of limbal stem cells*. Regen Med, 2013. **8**(5): p. 553-67.

33. EMA, E.M.A. *Holoclar*. [Website] 2015 [cited 2022 January]; Available from: https://www.ema.europa.eu/en/medicines/human/EPAR/holoclar.

34. Pellegrini, G., et al., *Navigating Market Authorization: The Path Holoclar Took to Become the First Stem Cell Product Approved in the European Union*. Stem Cells Transl Med, 2018. **7**(1): p. 146-154.

35. Rheinwald, J.G. and H. Green, *Serial cultivation of strains of human epidermal keratinocytes: the formation of keratinizing colonies from single cells*. Cell, 1975. **6**(3): p. 331-43.

36. Sun, T.T. and H. Green, *Cultured epithelial cells of cornea, conjunctiva and skin: absence of marked intrinsic divergence of their differentiated states*. Nature, 1977. **269**(5628): p. 489-93.

37. Zambruno, G., et al., *Transforming growth factor-beta 1 modulates beta 1 and beta 5 integrin receptors and induces the de novo expression of the alpha v beta 6 heterodimer in normal human keratinocytes: implications for wound healing*. J Cell Biol, 1995. **129**(3): p. 853-65.

38. Matthyssen, S., et al., *Corneal regeneration: A review of stromal replacements*. Acta Biomater, 2018. **69**: p. 31-41.

39. Simpson, F., et al., *Regenerative medicine in the cornea*, in *Principles of regenerative medicine*. 2019, Elsevier. p. 1115-1129.

40. Brovold, M., et al., *Naturally-Derived Biomaterials for Tissue Engineering Applications*. Adv Exp Med Biol, 2018. **1077**: p. 421-449.

41. WHO, W.H.O. *GLOBAL DATA ON VISUAL IMPAIRMENTS 2010*. 2010 [cited 2022 January]; Available from: https://www.who.int/blindness/GLOBALDATAFINALforweb.pdf.

42. WHO, W.H.O. *Universal eye health: a global action plan 2014-2019*. 2013 [cited 2022 January]; Available from: https://www.who.int/blindness/AP2014_19_English.pdf.

43. Gain, P., et al., *Global Survey of Corneal Transplantation and Eye Banking*. JAMA Ophthalmol, 2016. **134**(2): p. 167-73.

44. The Lewin Group, I., *Cost-Benefit Analysis of Corneal Transplant*. 2013. p. 24.

45. Ahearne, M., et al., *Designing scaffolds for corneal regeneration*. Advanced Functional Materials, 2020. **30**(44): p. 1908996.

46. El-Ayoubi, R., et al., *Design and dynamic culture of 3D-scaffolds for cartilage tissue engineering*. J Biomater Appl, 2011. **25**(5): p. 429-44.

47. Rama, P., et al., *Autologous fibrin-cultured limbal stem cells permanently restore the corneal surface of patients with total limbal stem cell deficiency*. Transplantation, 2001. **72**(9): p. 1478-85.

48. Mobaraki, M., et al., *Corneal Repair and Regeneration: Current Concepts and Future Directions*. Front Bioeng Biotechnol, 2019. **7**: p. 135.

49. Tsai, R.J., L.M. Li, and J.K. Chen, *Reconstruction of damaged corneas by transplantation of autologous limbal epithelial cells*. N Engl J Med, 2000. **343**(2): p. 86-93.

50. Neuman, M.G., et al., *Hyaluronic acid and wound healing*. Journal of pharmacy & pharmaceutical sciences, 2015. **18**(1): p. 53-60.

51. Zhong, J., et al., *Hyaluronate acid-dependent protection and enhanced corneal wound healing against oxidative damage in corneal epithelial cells*. Journal of ophthalmology, 2016. **2016**.

52. Gronkiewicz, K.M., et al., *Effects of topical hyaluronic acid on corneal wound healing in dogs: a pilot study*. Veterinary ophthalmology, 2017. **20**(2): p. 123-130.

53. Chen, Z., et al., *Biomaterials for corneal bioengineering*. Biomed Mater, 2018. **13**(3): p. 032002.

54. Guan, L., et al., *Use of a silk fibroin-chitosan scaffold to construct a tissue-engineered corneal stroma*. Cells Tissues Organs, 2013. **198**(3): p. 190-7.

55. Arasukumar, B., et al., *Chemical composition, structural features, surface morphology and bioactivities of chitosan derivatives from lobster (Thenus unimaculatus) shells*. Int J Biol Macromol, 2019. **135**: p. 1237-1245.

56. Zeng, J.B., et al., *Chitin whiskers: an overview*. Biomacromolecules, 2012. **13**(1): p. 1-11.

57. Yang, T.L., *Chitin-based materials in tissue engineering: applications in soft tissue and epithelial organ*. Int J Mol Sci, 2011. **12**(3): p. 1936-63.

58. Lanzalaco, S. and E. Armelin, *Poly(N-isopropylacrylamide) and Copolymers: A Review on Recent Progresses in Biomedical Applications*. Gels, 2017. **3**(4).

59. Roy, D., W.L. Brooks, and B.S. Sumerlin, *New directions in thermoresponsive polymers*. Chem Soc Rev, 2013. **42**(17): p. 7214-43.

60. Lee, S.G., et al., *Enhanced cell affinity of poly (d, l-lactic-co-glycolic acid)(50/50) by plasma treatment with β-(1→ 3)(1→ 6)-glucan*. Surface and Coatings Technology, 2007. **201**(9-11): p. 5128-5131.

61. Manavitehrani, I., et al., *Biomedical Applications of Biodegradable Polyesters*. Polymers (Basel), 2016. **8**(1).

62. Yañez-Soto, B., et al., *Biochemically and topographically engineered poly(ethylene glycol) diacrylate hydrogels with biomimetic characteristics as substrates for human corneal epithelial cells*. J Biomed Mater Res A, 2013. **101**(4): p. 1184-94.

63. Isaacson, A., S. Swioklo, and C.J. Connon, *3D bioprinting of a corneal stroma equivalent*. Exp Eye Res, 2018. **173**: p. 188-193.

64. Zhang, X. and Y. Zhang, *Tissue Engineering Applications of Three-Dimensional Bioprinting*. Cell Biochem Biophys, 2015. **72**(3): p. 777-82.

65. Zhang, B., et al., *3D bioprinting for artificial cornea: Challenges and perspectives*. Med Eng Phys, 2019. **71**: p. 68-78.

66. Ruiz-Alonso, S., et al., *Current Insights Into 3D Bioprinting: An Advanced Approach for Eye Tissue Regeneration*. Pharmaceutics, 2021. **13**(3).

67. Fuest, M., et al., *Prospects and Challenges of Translational Corneal Bioprinting*. Bioengineering (Basel), 2020. **7**(3).

68. Hinderer, S., S.L. Layland, and K. Schenke-Layland, *ECM and ECM-like materials - Biomaterials for applications in regenerative medicine and cancer therapy*. Adv Drug Deliv Rev, 2016. **97**: p. 260-9.

69. Joyce, K., et al., *Bioactive potential of natural biomaterials: identification, retention and assessment of biological properties*. Signal Transduct Target Ther, 2021. **6**(1): p. 122.

70. Uchida, N., et al., *Nanometer-sized extracellular matrix coating on polymer-based scaffold for tissue engineering applications*. J Biomed Mater Res A, 2016. **104**(1): p. 94-103.

71. Jia, L., C.E. Ghezzi, and D.L. Kaplan, *Optimization of silk films as substrate for functional corneal epithelium growth*. J Biomed Mater Res B Appl Biomater, 2016. **104**(2): p. 431-41.

72. Iturriaga-Goyon, E., et al., *Future Perspectives of Therapeutic, Diagnostic and Prognostic Aptamers in Eye Pathological Angiogenesis*. Cells, 2021. **10**(6).

73. Hasegawa, H., et al., *Methods for Improving Aptamer Binding Affinity*. Molecules, 2016. **21**(4): p. 421.

74. Miller, D.D., et al., *Recurrent corneal erosion: a comprehensive review*. Clin Ophthalmol, 2019. **13**: p. 325-335.

75. Simpson, F.C., et al., *Collagen analogs with phosphorylcholine are inflammation-suppressing scaffolds for corneal regeneration from alkali burns in mini-pigs*. Communications biology, 2021. **4**(1): p. 1-15.

76. Di Iorio, E., et al., *Q-FIHC: quantification of fluorescence immunohistochemistry to analyse p63 isoforms and cell cycle phases in human limbal stem cells*. Microsc Res Tech, 2006. **69**(12): p. 983-91.

77. Builles, N., et al., *Use of magnetically oriented orthogonal collagen scaffolds for hemi-corneal reconstruction and regeneration*. Biomaterials, 2010. **31**(32): p. 8313-22.

78. Ruscito, A. and M.C. DeRosa, *Small-Molecule Binding Aptamers: Selection Strategies, Characterization, and Applications*. Front Chem, 2016. **4**: p. 14.

79. Cerchia, L., et al., *Cell-specific aptamers for targeted therapies*. Methods Mol Biol, 2009. **535**: p. 59-78.

80. Ogawa, A., et al., *Aptamer selection for the inhibition of cell adhesion with fibronectin as target*. Bioorg Med Chem Lett, 2004. **14**(15): p. 4001-4.

81. Galli, C., et al., *Improved scaffold biocompatibility through anti-Fibronectin aptamer functionalization*. Acta Biomater, 2016. **42**: p. 147-156.

82. Ozeki, Y., T. Matsui, and K. Titani, *Cell adhesive activity of two animal lectins through different recognition mechanisms*. FEBS letters, 1991. **289**(2): p. 145-147.

83. Organization, W.H., *World report on vision*. 2019.

84. Chandra, P.K., S. Soker, and A. Atala, *Tissue engineering: Current status and future perspectives*, in *Principles of tissue engineering*. 2020, Elsevier. p. 1-35.

85. Karamichos, D., *Ocular tissue engineering: current and future directions*. Journal of Functional Biomaterials, 2015. **6**(1): p. 77-80.

86. Lin, L. and X. Jin, *The development of tissue engineering corneal scaffold: Which one the history will choose*. Ann Eye Sci, 2018. **3**: p. 1-8.

87. Jangamreddy, J.R., et al., *Short peptide analogs as alternatives to collagen in pro-regenerative corneal implants*. Acta biomaterialia, 2018. **69**: p. 120-130.

88. Hynes, R.O., *Integrins: bidirectional, allosteric signaling machines*. Cell, 2002. **110**(6): p. 673-87.

89. Parisi, L., et al., *Anti-fibronectin aptamers improve the colonization of chitosan films modified with D-(+) Raffinose by murine osteoblastic cells*. J Mater Sci Mater Med, 2017. **28**(9): p. 136.